LONG-TERM X-RAY LUMINOSITY AND ROTATIONAL EVOLUTION OF ACCRETING MILLISECOND X-RAY PULSARS

by
FATMANUR ERTUĞRUL

Submitted to the Graduate School of Engineering and Natural Sciences
in partial fulfilment of
the requirements for the degree of Master of Science

Sabancı University
July 2025

LONG-TERM X-RAY LUMINOSITY AND ROTATIONAL EVOLUTION OF ACCRETING MILLISECOND X-RAY PULSARS

Approved by:

Prof. ÜNAL ERTAN .....
(Thesis Supervisor)

Assoc. Prof. AYŞE ULUBAY .....

Prof. EMRAH KALEMCİ .....

Date of Approval: July 18, 2025

ABSTRACT

LONG-TERM X-RAY LUMINOSITY AND ROTATIONAL EVOLUTION OF ACCRETING MILLISECOND X-RAY PULSARS

FATMANUR ERTUĞRUL

Physics M.Sc. Thesis, July 2025

Thesis Supervisor: Prof. ÜNAL ERTAN

Keywords: accretion, accretion discs, neutron stars, accreting millisecond X-ray pulsars

Accreting millisecond X-ray pulsars (AMXPs) are neutron stars in low mass X-ray binaries (LMXBs). They spun-up through mass accretion from their companion. To date, 26 AMXPs including three transitional millisecond pulsars have been observed with spin periods shorter than 10 ms. All known AMXPs are transient sources likely to be in the final stages of the LMXB evolution, showing periodic X-ray pulses during their outbursts. It is important to study the rotational evolution of AMXPs since there are uncertainties in the disc-field interaction and torque mechanisms leading these sources to their descendants namely the radio millisecond pulsars. Observations show that the average torques acting on these systems during their long-term evolution are spin-down torques. In some conventional models, observed long-term spin-down behaviour of AMXPs require external spin-down torques, like gravitational radiation, in addition to disc and magnetic dipole torques. In this thesis, we investigate the torques acting on the AMXPs during their outburst and quiescent states. We use observational data of five AMXPs which have been observed during more than one outburst and have spin period derivative measurements for both outburst and quiescent states. We have found that the spin-up torques during the shorter outbursts are dominated by the spin-down torques during the much longer quiescent states, resulting in a net spin-down in their long-term transient evolution. Our model results are consistent with the observed X-ray luminosities and rotational properties of these five sources, which indicate that the long-term rotational evolution of AMXPs can be reproduced by the accretion torque, disc (magnetic) torque, and magnetic dipole torque, without invoking any additional external torque mechanisms.

ÖZET

KÜTLE AKTARAN MİLİSANİYE X-IŞINI PULSARLARININ UZUN DÖNEM X-IŞINI PARLAKLIĞI VE DÖNME EVRİMİ

FATMANUR ERTUĞRUL

Fizik Yüksek Lisans Tezi, Temmuz 2025

Tez Danışmanı: Prof. Dr. ÜNAL ERTAN

Anahtar Kelimeler: kütle aktarımı, kütle aktarım diskleri, nötron yıldızları, kütle aktaran milisaniye X-ışını pulsarları

Kütle aktaran milisaniye X-ışını pulsarları (AMXPs), düşük kütleli X-ışını çiftlerinde (LMXBs) bulunan ve eş yıldızından madde aktarımıyla hızlanmış olan nötron yıldızlarıdır. Bugüne kadar, dönme periyotları 10 ms'den düşük olan, üçü geçişken milisaniye pulsarı olmak üzere 26 AMXP gözlenmiştir. Bilinen tüm AMXP'ler büyük ihtimalle LMXB evriminin son evrelerinde bulunan geçişli kaynaklardır ve parlama zamanlarında periyodik X-ışını atmaları gösterirler. AMXP'lerin radyo milisaniye pulsarlarına dönüşmesini sağlayan disk-alan etkileşimi ve tork mekanizmalarında bulunan belirsizlikler nedeniyle dönme evrimini çalışmak önemlidir. Gözlemler, bu kaynakları uzun dönem evrimlerinde etkileyen ortalama torkların yavaşlama torkları olduğunu göstermiştir. Bazı geleneksel modellerde, AMXP'lerin gözlemlenen uzun dönem yavaşlama davranışı, disk ve manyetik dipol torkarına ek olarak kütleçekimsel ışınım gibi dış yavaşlama torkları gerektirir. Biz bu tezde AMXP'leri parlama ve durgun dönemlerinde etkileyen torkları inceledik. Birden fazla parlama döneminde gözlenmiş ve hem parlama hem de durgun zamanda dönme periyodu türevi ölçülmüş beş AMXP'nin gözlemsel verilerini kullandık. Daha kısa süren parlama dönemlerinde etkin olan hızlanma torklarının, çok daha uzun durgunluk zamanlarındaki yavaşlama torkları tarafından baskılandığını ve bunun sonucu olarak uzun dönem geçişli evrimlerinde yavaşladıklarını gösterdik. Model sonuçlarımız bu beş kaynağın gözlenen X-ışını parlaklıkları ve dönme özellikleriyle uyumludur. Bu da AMXP'lerin uzun dönem dönme evriminin aktarım torku, disk (manyetik) torku, ve manyetik dipol torku ile, herhangi bir ek dış tork mekanizmasına gerek kalmadan açıklanabildiğini göstermektedir.

ACKNOWLEDGEMENTS

I would like to express my deepest gratitude to my supervisor, Prof. Ünal Ertan, for his continuous guidance, support, and encouragement throughout my master's studies. I also thank my thesis jury members, Prof. Emrah Kalemci and Assoc. Prof. Ayşe Ulubay, for their time and helpful feedback.

I acknowledge full scholarship from faculty of engineering and natural sciences of Sabancı University, and research support from TÜBİTAK (The Scientific and Technological Research Council of Turkey) through grant 123F083.

I am deeply grateful to my family, Sevgi, Murat, and Doğuş, for their endless love and unwavering belief in me. Their presence has always been my greatest source of support. I would also like to thank Tuna for always standing by my side and making life more bearable. Finally, I am thankful to all my friends for their support along the way.

To my beloved family,
for their endless love and support

TABLE OF CONTENTS

LIST OF TABLES

LIST OF FIGURES

LIST OF ABBREVIATONS

1. INTRODUCTION

Some parts of this chapter and Chapters 2, 3, 4, 5 are included in our work that has been submitted to a scientific journal.

Stars remain in hydrostatic equilibrium, the balance between the gravitational and the thermal pressure forces, during most of their lifetimes. In the final stages of stellar evolution, they exhaust their nuclear fuel, and thermal pressure can no longer balance the gravity. For massive stars ($M \gtrsim 10\ M_{\odot}$), this causes star's core to collapse, leading to a supernova explosion, which releases an enormous amount of energy ($\sim 10^{51}$ ergs) in a few seconds that lasts for weeks to months and ejects the outer layers of the star (Woosley & Weaver, 1986).

During the core collapse of a massive star, the density increases so much that it becomes energetically favourable for electrons to combine with protons via inverse $\beta-$decay to form neutrons. This process fills the star's core with neutrons, where neutron degeneracy pressure becomes the dominant force against the gravity. If this pressure is sufficient to balance the gravity, the core becomes a neutron star. If the mass of the core is greater than a critical value ($\sim 3\ M_{\odot}$), even the neutron degeneracy pressure cannot prevent the collapse and the core collapses into a black hole.

Neutron stars are the most compact objects observable in the universe. A typical neutron star has a mass $M \simeq 1\ M_{\odot}$ and a radius $R_{*} \sim 10$ km, which gives an extremely high average density of $\rho \sim 10^{15}$ g cm^{-3}. Due to conservation of angular momentum during the core collapse, neutron stars can achieve extremely short spin periods, P, ranging from milliseconds to seconds. They also born with magnetic dipole fields with strength $B \sim 10^{12}$ G due to the magnetic flux conservation during the collapse.

The ideas about neutron stars came soon after the discovery of the neutron by Chadwick (1932). In the following year, Sterne (1933) proposed that electrons combine with protons to form neutrons at very high densities, which is called inverse

$\beta-$decay. He estimated the minimum mass density required for neutron abundance as $\rho \geq 2.3 \times 10^{10}$ g cm^{-3}. Sterne couldn't realize the possibility that these densities could be reached in astrophysical systems. The name of "neutron star" was coined by Baade and Zwicky in 1934. They suggested that ordinary stars become neutron stars during the supernova explosions, but could not explained the reason behind this process (Baade & Zwicky, 1934). In 1936, Gamow made the connection between neutron physics and astrophysical objects by proposing that massive stars, after exhausting all their nuclear fuel, form neutron cores through inverse $\beta-$decay (Gamow & Teller, 1936). Oppenheimer and Volkoff calculated the structure of neutron stars by considering the general relativistic effects and assuming non-interacting neutrons. They estimated the mass limit for a stable neutron star as 0.7 $M_{\odot}$ (Oppenheimer & Volkoff, 1939). When neutron-neutron interaction taken into account, the mass limit increased to 2 $M_{\odot}$ (Cameron, 1959).

After almost 30 years of theoretical work, a radio pulsar (PSR 1919+21) with $P =$ 1.377 s was observed by Jocelyn Bell in 1967 for the first time (Hewish et al., 1968). The fact that the pulses are so frequent and stable indicated that the source cannot be a normal star, it must be a compact star. The following detection of new pulsars and analysis showed that these systems, which cannot be white dwarfs either, are neutron stars. Since the discovery of Bell, more than 3700 radio pulsars were detected (ATNF Pulsar Catalogue, version 2.6.3, Manchester et al., 2005)[1].

In 1965, Zel'dovich & Novikov emphasized the significance of the accretion processes in compact objects, and argued that mass accretion on to neutron stars and black holes can be converted into radiation energy more efficiently than in the fusion reactions. The first X-ray pulsar Sco X-1 was observed in 1962 during a rocket flight designated to observe X-rays from the lunar surface (Giacconi et al., 1962). It was classified as an X-ray source but the significance of the source as an accreting X-ray pulsar was not recognized until the first X-ray satellite, UHURU, was launched in 1970. UHURU scanned the sky in X-rays, preparing an X-ray survey and paved the way for the discovery of binary X-ray pulsars. In a short time after the launch, Cen X-3 with $P = 4.84$ s (Giacconi et al., 1971) and Her X-1 with $P = 1.24$ s (Tananbaum et al., 1972) were discovered.

Rapidly rotating neutron stars with a strong magnetic field generate very strong electric potentials that can accelerate charged particles along the magnetic field lines emerging from the poles of the star. This creates beams of radiation from radio to gamma rays which is emitted from the magnetic poles of the star. Since magnetic and rotation axes of a neutron star are usually misaligned, the radiation

[1] https://www.atnf.csiro.au/research/pulsar/psrcat/

beams sweep out the sky as the star rotates. If one of these radiation beams cross our position, we receive regular pulses with a period equal to the rotational period of the star.

Neutron stars can also emit periodic X-ray pulses when the magnetic dipole field lines channel the accretion to the poles of the star. The accretion on to a neutron star converts the rest mass energy into radiation approximately thirty times more efficiently than nuclear fusion reactions (Frank et al., 2002). The kinetic energy of accreted material is converted into heat through dissipative processes on the surface of the star. The resulting X-ray luminosity, $L_{\rm X} = GM\dot{M}_*/R_*$, where $\dot{M}_*$ is the mass-flow rate on to the star and G is the gravitational constant. The mass flow on to the magnetic poles heats up the polar caps, which produces pulsed X-ray emission due to the rotation of the star.

Most of the accretion powered pulsars are members of binary star systems. In X-ray Binaries (XRBs), a neutron star or a black hole accretes matter from a companion star. They are classified according to the mass of the companion star: high mass X-ray binaries (HMXBs) contain a young massive donor often exceeding 10 $M_\odot$, and low mass X-ray binaries (LMXBs) have an older donor star with a mass smaller than 1 $M_\odot$. In HMXBs, the compact object usually accretes matter from the wind of the massive companion. Roche lobe overflow is the main mass transfer mechanism in LMXBs, which forms a geometrically thin accretion disc around the neutron star. The sources that we analyse in this thesis belong to the LMXB class.

In Roche lobe overflow, the outer layers of the donor star are pulled into the gravitational field of the neutron star as the binary separation decreases, or as the radius of the companion star expands to fill its Roche lobe. Companion matter flowing through the first Lagrangian (L_1) point spirals into an eccentric orbit before falling into the neutron star. The matter eventually settles down in a circular orbit through viscous dissipative processes which also spreads the continuously flowing matter both outwards and inwards forming an accretion disc (for more details, see Frank et al. 2002).

Accretion on to neutron star is possible when the inner disc radius, $r_{\rm in}$, is equal to or smaller than the co-rotation radius, $r_{\rm co} = (GM/\Omega_*^2)^{1/3}$, at which the angular velocity of the star, Ω_*, is equal to the Keplerian angular velocity of the disc matter, $\Omega_{\rm K}$. In this state, star spins up. When $r_{\rm in} > r_{\rm co}$, star enters the propeller phase where all the inflowing matter expelled from the system and star spins down. In conventional models, $r_{\rm in}$ is estimated by equating the magnetic and viscous stresses and found to be close to the Alfvén radius, $r_{\rm A} \simeq (GM)^{-1/7}\ \mu^{4/7}\ \dot{M}_{\rm in}^{-2/7}$, where μ is the magnetic dipole moment of the star and $\dot{M}_{\rm in}$ is the mass-inflow rate of the

disc (Davidson & Ostriker, 1973). With a constant $\xi \sim 0.5-1$, $r_{\rm in} = \xi\ r_{\rm A}$ (Ghosh & Lamb, 1979).

LMXBs are classified as either persistent or transient depending on the stability of the disc and $\dot{M}_{\rm in}$ at the inner disc. Persistent sources are observed with nearly stable X-ray luminosities around $L_{\rm X} \sim 10^{35} - 10^{38}$ erg s^{-1}. LMXBs become transient below a critical $\dot{M}_{\rm in}$ level, depending on the orbital period of the binary. Transient sources alternate between quiescence that lasts months to years with $L_{\rm X} \sim 10^{31} - 10^{33}$ erg s^{-1} and outburst intervals lasting weeks to months with $L_{\rm X} \sim 10^{35} - 10^{38}$ erg s^{-1} (Dubus et al., 1999).

This transient behaviour is explained by the disc instability model (DIM), originally developed for dwarf novae and later adapted to transient low-mass X-ray binaries (Dubus et al., 1999; Lasota, 2001). According to this model, the transient behaviour is produced by the viscous instabilities in the disc. When the effective temperature of the disc, $T_{\rm eff}$, is below the hydrogen ionization temperature, the disc remains in a cold and low-viscosity state. The mass accumulates at the outer region of the disc in this state. With increasing surface density, $T_{\rm eff}$ increases above the hydrogen ionization temperature and the disc transitions to a hot and high-viscosity state. In this state, the matter is transferred more efficiently inwards. The instability is triggered locally at a radial distance of the disc. If the resultant heating front propagating inner and outer radii, takes all or most of the disc into the hot state, which is observed as an X-ray outburst due to enhanced mass flow inwards. Surface densities decrease rapidly in the outburst state. Starting from the outer disc regions, surface density decrease below the critical value causing transition back to the cold state. The cooling front propagating inward with the sound speed take the system into the cold state, and thus into the quiescence.

It was realized that the X-ray irradiation of the disc is very important in that its strength determines whether a given source could remain persistent. The X-ray irradiation flux, $F_{\rm irr}$, prevent the inward propagation of the cooling front in the hot state. If this heating mechanism keeps the entire disc in the hot state, then the system is observed as a persistent LMXB. Depending on the outer radius, $r_{\rm out}$, of the disc, there is a critical $\dot{M}_{\rm in}$ for $F_{\rm irr}$ to keep the entire disc in the hot viscosity state. If the mass-flow rate from the companion is below this critical $\dot{M}_{\rm in}$ level, then the system is observed as a transient X-ray source (see Dubus et al., 1999; Lasota, 2001 for a review of disc instability model)

During the long-term evolution, LMXBs become transient likely during their Roche-lobe decoupling phase. All known accreting millisecond X-ray pulsars (AMXPs) are transient LMXB sources that exhibit coherent X-ray pulsations with periods in the

millisecond range. While not all transient sources are AMXPs, all AMXPs are transient. It is important to understand the rotational evolution of AMXPs since they are the only LMXBs with observable X-ray pulses and timing properties. They provide a direct evidence for the recycling scenario in which an old neutron star gradually gains angular momentum as it accretes matter from the companion star and eventually becomes a millisecond pulsar (Alpar et al., 1982; Radhakrishnan & Srinivasan, 1982). The discovery of SAX J1808.4−3658 in 1998 with $P = 2.5$ ms offered the first observational support of the recycling scenario (Wijnands & van der Klis, 1998). Further support to this idea came with the discovery of three transitional millisecond pulsars (tMSPs), which switch between X-ray pulsar and radio pulsar states. These sources are very likely the evolutionary link between AMXPs and radio millisecond pulsars (RMSPs). Fig. 1.1 shows these sources in the $P - \dot{P}$ diagram.

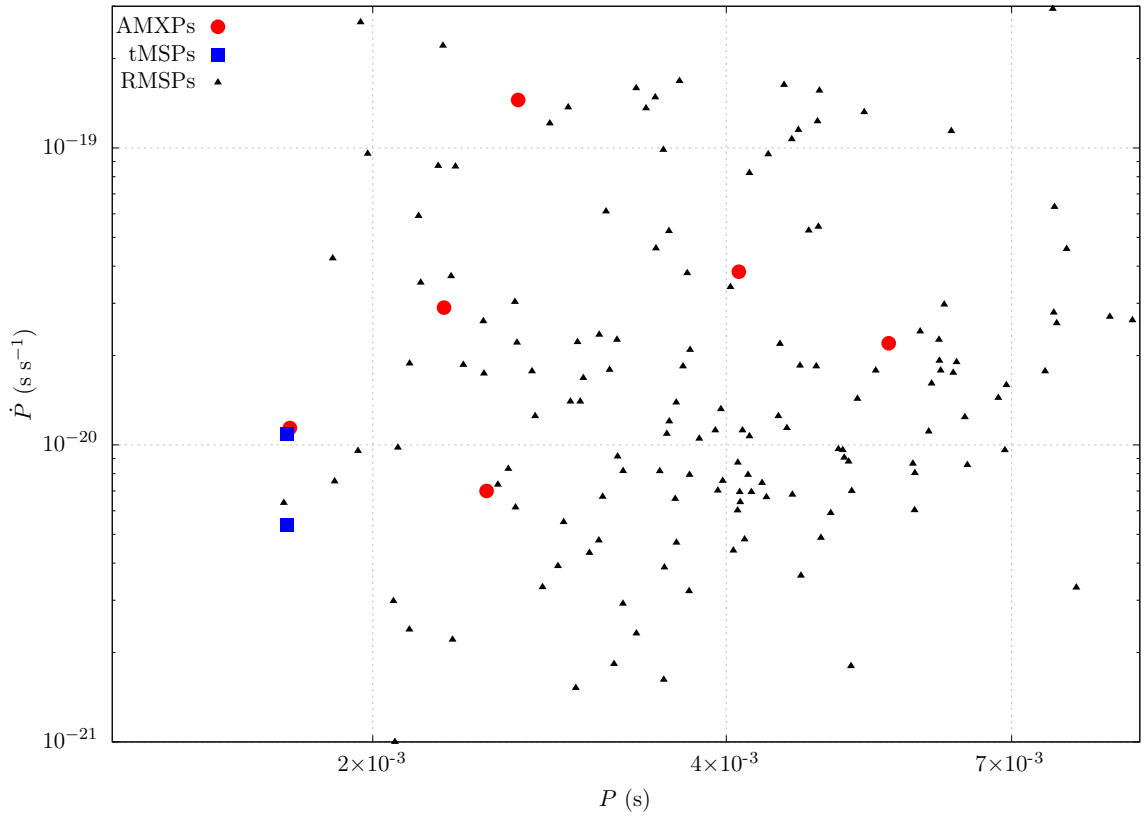

Figure 1.1 AMXPs in the $P - \dot{P}$ diagram. AMXPs with measured secular $\dot{P}$ are shown by red dots (Riggio et al., 2011a; Papitto et al., 2011; Bult et al., 2018; Ng et al., 2021; Sanna et al., 2025). Blue squares represent the two tMSPs (PSR J1023+0038 and XSS J1227−4859) which have estimated $\dot{P}$ during the quiescence (Papitto & Martino, 2022). RMSPs that are in a binary with $P < 10$ ms shown with black triangles. Data of RMSPs were taken from the online ATNF Pulsar Catalogue (version 2.6.3, Manchester et al., 2005, https://www.atnf.csiro.au/research/pulsar/psrcat/)

AMXPs exhibit coherent X-ray pulsations in the millisecond range during their

outbursts. Most of them are observed to spin up during the outburst through accretion. IGR J00291+5934 is the fastest AMXPs with $P = 1.7$ ms (Markwardt et al., 2004). It was the first source showed a net spin-up during outburst with a spin period derivative of $\dot{P} = -(1.42 \pm 0.08) \times 10^{-18}$ s s^{-1} (Papitto et al., 2011). So far, these X-ray pulsations were detected only during outbursts, which may indicate that there is no mass-flow on to the star in quiescence, or a weak accretion is present, but the pulsations remain undetectable due to low detection limits.

AMXPs stay in the quiescent state during most of their evolution, with no or little accretion on to the neutron star. Secular $\dot{P}$ is usually measured from the P measurements during successive outbursts. Only six AMXPs showed more than one outburst, which were XTE J1751−305, IGR J17494−3030, Swift J1756.9−2508, IGR J17511−3057, IGR J00291+5934, and SAX J1808.4−3658. For these sources, $\dot{P}$ values during the quiescence was measured, and found to be positive (Di Salvo & Sanna, 2022).

Observations of AMXPs indicate that spin-up during a short-lived outburst is not enough to compensate for the spin-down during the following long quiescent state. The long-term spin-down is likely to be a common property among the AMXPs. In the literature, inner disc is mostly assumed to be evaporated, preventing the disc-field interaction due to the very low $\dot{M}_{\rm in}$ levels during the quiescence. It is suggested that the neutron stars in some AMXPs slow down mainly by the magnetic dipole torques during the quiescent states. For these sources, the dipole field strength at the NS equator is estimated from the dipole torque formula as $B \simeq 3.2 \times 10^{19} \sqrt{P\ \dot{P}}$ G, using the measured P and $\dot{P}_{\rm secular}$. In this scenario, AMXPs are expected to emit radio pulses during this state. To date, only tMSPs were observed to switch between accretion and radio pulsar states, but no AMXPs showed radio pulsations during the quiescence, and it is still unclear what causes this difference between these two subclasses of LMXBs. If $\dot{M}_{\rm in}$ levels do not decrease sufficiently to truncate the disc during the quiescence, magnetic torque produced by the disc-field interaction becomes dominant. In this case, the dipole torque formula overestimates the B value.

In a recent study by Çoban & Ertan (2024), the typical outburst light curves of Aql X-1 were investigated based on the analytical torque model previously developed by Ertan (2017). The results of this study indicate that the mass accretion on to the neutron star goes on during the quiescence. This might happen since this source has a relatively high quiescent X-ray luminosity of $L_{\rm X} \sim 10^{33} - 10^{34}$ erg s^{-1} compared to other AMXPs. This might indicate that the disc-field interaction continues during the quiescent states as well at least for some AMXPs. This means that the dominant

spin-down torque is the disc torque rather than dipole torques in the quiescence. Ongoing low-level accretion might also be the reason for the lack of radio pulses during this state.

For persistent LMXBs, the rotational evolution of the neutron star can often be modelled using a long-term average $\dot{M}_{\rm in}$, assuming a relatively steady torque acting on the star. For transient systems such as AMXPs, $\dot{M}_{\rm in}$ varies drastically between the outburst and quiescent states. In such systems, the long-term rotational evolution estimated by the average $\dot{M}_{\rm in}$ is likely to be misleading. It was suggested that the transient nature of AMXPs allows for more efficient spin-up torques during outbursts, leading them to reach lower equilibrium spin periods compared to persistent sources that evolve under relatively steady $\dot{M}_{\rm in}$ (Bhattacharyya & Chakrabarty, 2017; D'Angelo, 2017). In these models, with relatively large difference between spin-up torques during the outburst state and spin-down torques acting during the quiescence, AMXPs are estimated to reach the sub-millisecond periods. Since, no such systems has been observed, external torque mechanisms, such as gravitational radiation, were suggested to be the mechanism preventing AMXPs from an efficient spin-up to sub-millisecond periods (Bhattacharyya & Chakrabarty, 2017).

In this thesis, we have investigated the long-term rotational evolution of AMXPs. To calculate $r_{\rm in}$ and resulting torques we used the analytical torque model developed by Ertan (2017, 2018) to calculate the inner disc radius, $r_{\rm in}$, in the propeller phase and explain the torque-luminosity behaviour of NSs. The model was later extended to include the all the rotational phases of NSs in LMXBs (Ertan, 2021). The model was used earlier to explain the torque reversals (Gençali et al., 2022) of LMXBs, and pulsed/non-pulsed behaviour of LMXBs (Niang et al., 2024). In Chapter 2, we present the details of the model. The source properties used in this study with the results of our calculations are given in Chapter 3. We discuss our results in Chapter 4, and summarise our conclusions in Chapter 5.

2. THE MODEL

Here we describe briefly the rotational phases and the transitions between these phases in the model for the neutron stars accreting from geometrically thin accretion discs (for details, see Ertan 2017, 2018, 2021). In the model, for sources evolving with steady $\dot{M}_{\rm in}$, there are three rotational phases: the strong-propeller (SP), the weak-propeller (WP), and the spin-up (SU) phase. These phases are determined by the current location of $r_{\rm in}$ with respect to $r_{\rm co}$, and there is not a single $r_{\rm in}$ formula for the three phases. Below we will summarize the properties and the transitions between these phases with increasing $\dot{M}_{\rm in}$.

At low $\dot{M}_{\rm in}$ levels, the system is in the SP phase. In this phase, the maximum inner disc radius at which the SP condition can be achieved is estimated as

$$R_{\rm in,max}^{25/8} \, |1 - R_{\rm in,max}^{-3/2}| \simeq 1.26 \; \alpha_{-1}^{2/5} \; M_{1.4}^{-7/6} \; \dot{M}_{\rm in,16}^{-7/20} \; \mu_{30} \; P^{-13/12} \tag{2.1}$$

where $R_{\rm in,max} = r_{\rm in,max}/r_{\rm co}$, $\alpha_{-1} = (\alpha/0.1)$ is the kinematic viscosity parameter, $M_{1.4} = (M/1.4 \;\; M_\odot)$, $\dot{M}_{\rm in,16} = (\dot{M}_{\rm in}/10^{16}{\rm g\ s^{-1}})$, and $\mu_{30} = (\mu/10^{30}\ {\rm G\ cm^3})$. We define $r_{\rm in} = r_\eta = \eta\ r_{\rm in,max}$ with $\eta \lesssim 1$, because of the sharp radial dependence of the magnetic torque. In a steady SP phase, $r_{\rm in} > r_1 = 1.26\ r_{\rm co}$. At radii larger than r_1 (point B in Fig. 3.1), the field-lines co-rotating with the star can accelerate the matter at the inner disc boundary to speeds exceeding the escape speed, $v_{\rm esc}$, and effectively expel from the system. In this phase, there is no mass accretion on to the neutron star and sources that have sufficient rotational power can emit ordinary radio pulses.

As $\dot{M}_{\rm in}$ increases, if $r_{\rm in}$ is instantaneously between r_1 and $r_{\rm co}$, the matter thrown out of the inner disc boundary falls back to the disc at larger radii. This causes pile-up of the matter in the disc, which pushes $r_{\rm in}$ to $r_{\rm co}$ until $r_{\rm in} = r_{\rm co}$ (from point B to D), at which the system enters the WP phase. In this phase, for a large range of $\dot{M}_{\rm in}$ (from point D to E), the system spins down with mass flow from $r_{\rm in} = r_{\rm co}$ along the closed field lines on to the neutron star surface, which is likely to quench the ordinary radio pulses.

With further increase in $\dot{M}_{\rm in}$, the viscous stresses dominate the magnetic stresses, and the inner disc penetrates into $r_{\rm co}$. This also corresponds to the WP/SU transition. This happen approximately when $r_\xi \simeq r_{\rm co}$ where $r_\xi = \xi\ r_{\rm A}$, $r_{\rm A}$ is the conventional Alfvén radius and ξ is a parameter close to unity. Beyond the $\dot{M}_{\rm in}$ level for this transition, $r_{\rm in}$ tracks r_ξ for a narrow $\dot{M}_{\rm in}$ range until it reaches the unstable, upper r_η (Equation 1) branch (from point E to F). When r_ξ crosses this unstable r_η, the inner disc moves inward, opening up the closed field lines until reaching the stable lower branch of r_η for the same $\dot{M}_{\rm in}$ value. As $\dot{M}_{\rm in}$ increases further, $r_{\rm in}$ tracks r_η until the disc reaches the surface of the neutron star (see point G in fig. 1 of Niang et al., 2024). In some cases, stable r_η could be smaller than $R_* \simeq 10^6$ cm. In this case, $r_{\rm in} = R_*$ (point H). For the five sources we investigate in this work, our results indicate that; $r_{\rm in}$ reaches R_* before the stable r_η branch (see Figs 3.1–3.5). To sum up, $r_{\rm in}$ is calculated using Equation (2.1) in both SP and SU phases except a narrow $\dot{M}_{\rm in}$ range during the torque reversal ($r_{\rm in} \simeq r_\xi$), while $r_{\rm in} = r_{\rm co}$ in the WP phase.

The total torque acting on the star can be written as:

$$\Gamma = \sqrt{GMr_{\rm in}}\dot{M}_* - \frac{\mu^2}{r_{\rm in}^3}\left(\frac{\Delta r}{r_{\rm in}}\right) - \frac{2\mu^2\Omega_*^3}{3c^3} \tag{2.2}$$

where the first term is the spin-up torque, $\Gamma_{\rm acc}$, associated with the accretion on to the star, and the second term is the spin-down torque, $\Gamma_{\rm D}$, arising from the interaction between the magnetic dipole field lines and the disc inside the boundary region with radial width $\Delta r < r$. The last term is the magnetic dipole torque, $\Gamma_{\rm dip}$, where c is the speed of light. $\Gamma_{\rm dip}$ is mostly negligible in the presence of $\Gamma_{\rm D}$ and $\Gamma_{\rm acc}$.

In the SP phase, $\dot{M}_* = 0$ thus $\Gamma_{\rm acc} = 0$, and the star slows down with $\Gamma = \Gamma_{\rm D} + \Gamma_{\rm dip}$. In the WP phase, all torques are active, while $\Gamma_{\rm D}$ mostly dominates both $\Gamma_{\rm acc}$ and $\Gamma_{\rm dip}$, and the system slows down. As sources evolve with $r_{\rm in} = r_{\rm co} < r_\xi$ (the WP phase), increasing $\dot{M}_{\rm in}$ causes $\Gamma_{\rm acc}$ to increase and eventually exceed $\Gamma_{\rm D}$ which is constant in this phase, causing a transition from the WP to the SU phase (torque reversal). In the SU phase, $\Gamma = \Gamma_{\rm acc} + \Gamma_{\rm dip}$.

3. THE SOURCES & RESULTS

For the 26 known AMXPs including the three tMSPs, $P < 10$ ms (Patruno & Watts, 2021; Papitto & Martino, 2022). Among these, $\dot{P}_{\rm secular}$ values were estimated for six sources, and found to be positive, that is, they spin down in the long term (Di Salvo & Sanna, 2022). This is likely to be the common property of most of the other AMXPs as well considering their long quiescent states with similar low $L_{\rm X}$ levels. In this work, we analyse the five of these six sources with observational properties given in Table 3.1. We exclude SAX J1808.4–3658 due to uncertainties in its $\dot{P}$ measurements (see e.g. Burderi et al., 2006; Di Salvo & Sanna, 2022 for a review). Among these AMXPs, the $\dot{P}_{\rm outburst}$ values were also measured for three sources and constrained for two sources (see Table 3.1). In our calculations, for comparison of a measured $\dot{P}_{\rm outburst}$ with the model prediction, we consider the $L_{\rm X}$ (and corresponding $\dot{M}_{\rm in}$) range for which this particular $\dot{P}_{\rm outburst}$ was measured.

The reasonable model curves for the five sources are given in Figs 3.1–3.5. Our results indicate that the systems could be in either the SP phase (panels a) or the WP phase (panels b) in the quiescence to account for their spin-down behaviour. For both phases, the spin-down torque arising from the disc-field interaction is dominant. While the accretion is allowed in the WP phase, all the inflowing matter at the inner disc is expelled out of the system in the SP phase. For each source, we also test the possibility that the inner disc could be truncated due to evaporation by thermal instabilities at low $\dot{M}_{\rm in}$ levels in the quiescent state (Frank et al., 2002). In this case, the source slows down with the magnetic dipole torque alone (panels c). The dipole fields estimated for the case of evaporated inner disc in the quiescent state are relatively strong by a factor of $\sim$ 2–7. For these different cases, the model can produce reasonable results in agreement with the observed source properties in both the quiescent and the outburst states without any need to an additional external torque mechanism.

Table 3.1 Properties of AMXPs

AMXP Name	P (ms)	$\dot{P}_{\rm outburst}$ (10^{-18} s s^{-1})	$\dot{P}_{\rm secular}$ (10^{-20} s s^{-1})	Pulsed $L_{\rm X}$ Interval (10^{36} erg s^{-1})	$L_{\rm X}$ (Quiescence) (10^{32} erg s^{-1})	Distance (kpc)	Ref.
XTE J1751−305	2.3	$-(1.96 \pm 0.53)$	2.9 ± 0.6	$2.7 - 27$	< 4.6	8.5	*a*
IGR J17494−3030	2.66	$< \lvert 12.7 \rvert$	14.5 ± 0.5	$0.0494 - 2.18$	< 10.4	8	*b*
Swift J1756.9−2508	5.5	$< \lvert 42.2 \rvert$	2.2 ± 0.78	$0.76 - 15.3$	< 10	8	*c*
IGR J17511−3057	4.1	$-(2.42 \pm 0.3)$	3.83 ± 1.83	$3 - 11$	4.39 ± 0.85	< 6.9	*d*
IGR J00291+5934	1.7	$-(1.42 \pm 0.08)$	1.14 ± 0.33	$0.327 - 8.05$	2.6 ± 1.6	4.2 ± 0.5	*e*

Note. *(a)* Markwardt et al. (2002); Wijnands et al. (2005); Gierliński & Poutanen (2005); Papitto et al. (2008); Riggio et al., (2011a); *(b)* Armas Padilla et al. (2013); Chakrabarty et al. (2013); Ng et al. (2021); *(c)* Krimm et al. (2007); Papitto et al. (2007); Sanna et al. (2018); Bult et al. (2018); Li et al. (2021); *(d)* Markwardt et al. (2009); Altamirano et al. (2010); Riggio et al., (2011b); Haskell et al. (2012); Sanna et al. (2025); *(e)* Markwardt et al. (2004); Jonker et al. (2005); Galloway et al. (2005); Papitto et al. (2011); De Falco et al. (2017)

3.1 XTE J1751–305

This source was discovered in 2002 with $P = 2.3$ ms (Markwardt et al., 2002). The distance to the source is estimated to be 8.5 kpc assuming it is located near the Galactic Centre (Gierliński & Poutanen, 2005). Its observed properties and the model curves are seen in Fig. 3.1. Coherent X-ray pulsations were detected during the first 9 days of the 2002 outburst (Papitto et al., 2008) during which $L_{\rm X}$ decreased from the peak level of 2.7×10^{37} erg s^{-1} to 2.7×10^{36} erg s^{-1} (Gierliński & Poutanen, 2005; orange shaded area in the SU region). For this $L_{\rm X}$ range, $\dot{P}_{\rm outburst} = -(1.96 \pm 0.53) \times 10^{-18}$ s s^{-1} (Papitto et al., 2008; horizontal dotted line segment). Close to the $L_{\rm X}$ peak of the 2002 outburst, $\dot{P} = -(2.95 \pm 0.63) \times 10^{-18}$ s s^{-1} (Papitto et al., 2008; red data point with error bars). Due to the low $L_{\rm X}$ levels and short durations in the 2005 and 2007 outbursts, the P variations could not be measured. The P measurements at the end of the 2002 outburst and at the beginning of the 2009 outburst give $\dot{P}_{\rm secular} = (2.90 \pm 0.6) \times 10^{-20}$ s s^{-1} (Riggio et al., 2011a; horizontal dot-dot-dashed line segment). The $L_{\rm X}$ upper limit for the quiescent state is 4.6×10^{32} erg s^{-1} (Wijnands et al., 2005; vertical dashed line with arrows).

It is seen in Fig. 3.1 that the source could be in the SP phase (Fig. 3.1a) or possibly in the WP phase (Fig. 3.1b) during the quiescent state, depending on $\dot{M}_{\rm in}$ and B. An illustrative model curve in Fig. 3.1a is obtained with $B \simeq 1.0 \times 10^8$ G reproduces the observed $\dot{P}_{\rm secular}$ at $\dot{M}_{\rm in} \simeq 2.85 \times 10^{11}$ g s^{-1} while the source is in the SP phase (no mass accretion). Since the actual $L_{\rm X}$ level during the quiescence is unknown, the model cannot constrain the $B - \dot{M}_{\rm in}$ pair that reproduces the observed $\dot{P}_{\rm secular}$. Lower $\dot{M}_{\rm in}$ levels require lower B values. In Fig. 3.1b, the source is in the WP phase (accretion allowed) in the quiescent state. In this case, the observed $\dot{P}_{\rm secular}$ requires $B \simeq 6.0 \times 10^7$ G. For both possibilities in the quiescence, the abrupt rise in $\dot{M}_{\rm in}$ during the outburst, takes the source into the SU phase.

We also consider the possibility that the inner disc could be evaporated in the quiescent state (Fig. 3.1c). In this case, the spin down with dipole torques can account for the measured $\dot{P}_{\rm secular}$ with $B \simeq 2.6 \times 10^8$ G. It is not easy to estimate the location of $r_{\rm in}$ when the inner region of the disc is evaporated. We simply neglect $\Gamma_{\rm D}$ in our calculations for the evaporated state. We assume that the inner disc forms again and the source enters the SU phase with sharply increasing $\dot{M}_{\rm in}$ during the outburst.

For about a 7-year quiescence, XTE J1751−305 showed a spin-down of $\Delta P \simeq 6.4 \times 10^{-12}$ s, corresponding to $\dot{P}_{\rm secular} = (2.90 \pm 0.6) \times 10^{-20}$ s s^{-1}. During its 9-day

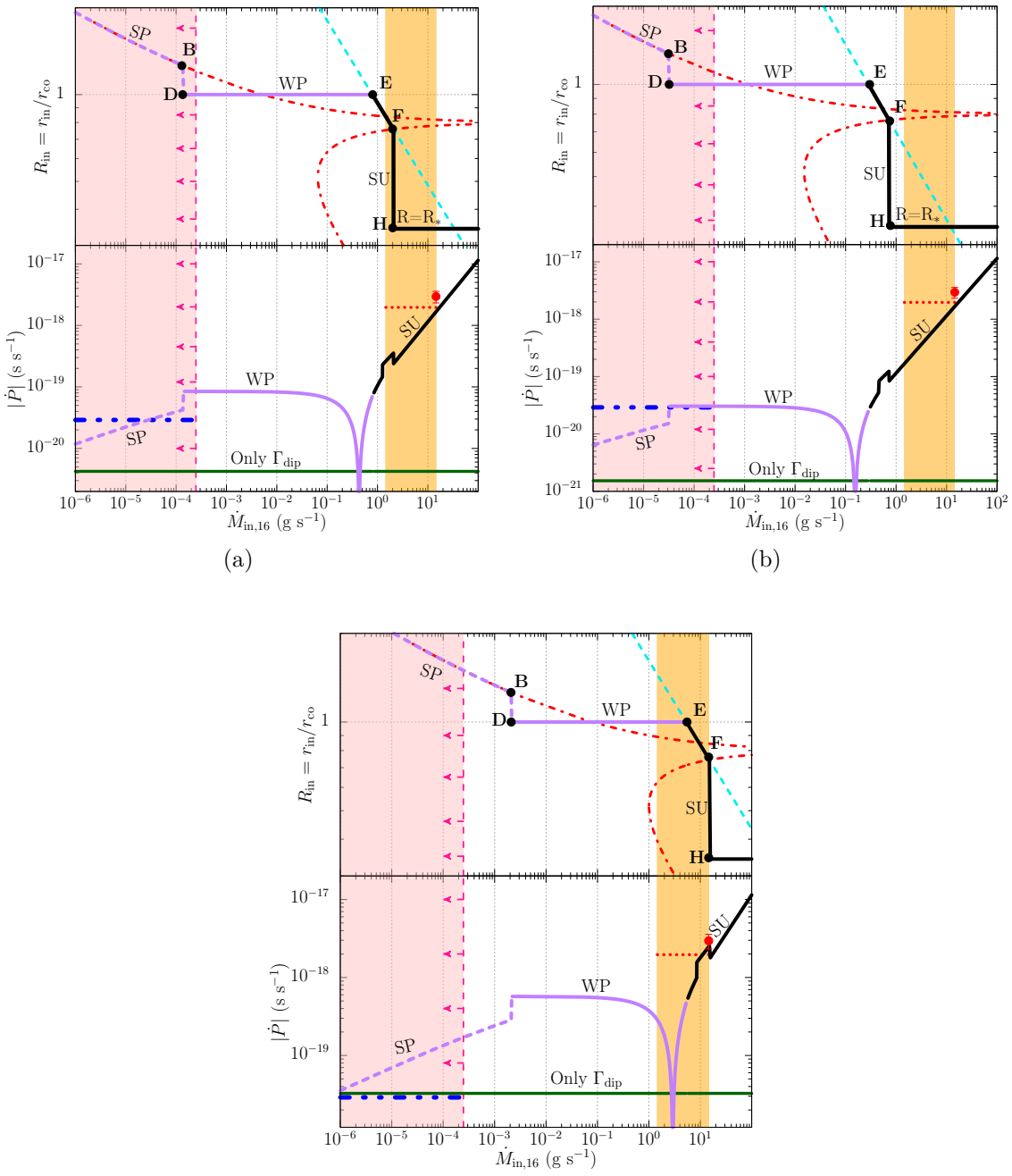

Figure 3.1 The model curves for XTE J1751−305. (a) $R_{\rm in}$ (top) and $\dot{P}$ (bottom) variation with $\dot{M}_{\rm in}$ across the SP (dashed purple), WP (solid purple), and SU (black) phases. Parameters: $P = 2.3$ ms, $\Delta r/r_{\rm in} = 0.25$, $\eta = \xi = 0.8$. Top: red dot-dashed and turquoise dashed lines indicate R_η and R_ξ, respectively. Bottom: red dotted and blue dot-dot-dashed lines show observed $\dot{P}_{\rm outburst}$ (negative) and $\dot{P}_{\rm secular}$ (positive). The dark-green continuous line represents the $\dot{P}$ calculated only with $\Gamma_{\rm dip}$ in the model. Vertical dashed line with arrows represents the upper limit on quiescent $\dot{M}_{\rm in}$; orange area shows pulsed $\dot{M}_{\rm in}$ range observed during the outburst. The red dot with error bars shows the measured $\dot{P}$ value at the peak of the 2002 outburst. These model curves are obtained with $B \simeq 1.0 \times 10^8$ G. (b) The same as (a) except $B \simeq 6.0 \times 10^7$ G. (c) The same as (a) except the dipole field $B \simeq 2.6 \times 10^8$ G is calculated from the dipole-torque formula with measured P and $\dot{P}_{\rm secular}$ in the quiescent state.

outburst, the source spun up with $\Delta P \simeq -1.7 \times 10^{-12}$ s corresponding to $\dot{P}_{\rm outburst} = -(1.96 \pm 0.53) \times 10^{-18}$ s s^{-1}. This indicates that the spin-up during outbursts is dominated by the spin-down during quiescent states.

For XTE J1751−305, our results do not eliminate (or favour) the evaporation of the inner disc in the quiescence. Detection of X-rays in the quiescent state could better constrain the models. In all three possibilities, the illustrative model curves could reproduce the observed $\dot{P}_{\rm outburst}$ and the $\dot{P}$ value measured at the peak of the outburst. We note that the $\dot{P}$ values in the model are estimated for the sources with steady $\dot{M}_{\rm in}$ levels. For instance, propagation of the inner disc during the rise and decay phases of the outbursts, and the resultant time dependent effects are not addressed in the model. For our aim, it is sufficient to roughly produce the measured outburst $\dot{P}$ levels.

3.2 IGR J17494–3030

This source was discovered in 2012 (Boissay et al., 2012; Armas Padilla et al., 2013). The distance to the source is estimated to be 8 kpc assuming it is located close to the Galactic Centre (Armas Padilla et al., 2013). The observed properties and the model curves for this source are seen in Fig. 3.2. Two outburst in 2012 and 2020 have been observed from this source with similar $L_{\rm X}$ levels (Ng et al., 2021). The coherent X-ray pulses with $P = 2.66$ ms were detected throughout the second outburst (Ng et al., 2020) during which $L_{\rm X}$ decreased from 2.18×10^{36} erg s^{-1} to 4.94×10^{34} erg s^{-1} (Ng et al., 2021; orange shaded area in the SU region). For this $L_{\rm X}$ range, the upper limit on $|\dot{P}_{\rm outburst}| < 1.27 \times 10^{-17}$ s s^{-1} (Ng et al., 2021; horizontal dotted line segment with arrows). Only after reanalysing the archived data of the 2012 outburst, the X-rays pulses were recovered, during which $L_{\rm X} \sim 1.7 \times 10^{35}$ erg s^{-1} (Armas Padilla et al., 2013), allowing the estimation of $\dot{P}_{\rm secular} = (1.45 \pm 0.05) \times 10^{-19}$ s s^{-1} (Ng et al., 2021; horizontal dot-dot-dashed line segment). For quiescence, $L_{\rm X} < 1.04 \times 10^{33}$ erg s^{-1} (Chakrabarty et al., 2013; vertical dashed line with arrows).

For the quiescent state, reasonable model curves are obtained when the model sources is in both the SP phase (see Fig. 3.2a) and the WP phase (see Fig. 3.2b). The model reproduces the measured $\dot{P}_{\rm secular}$ with $B \simeq 3.0 \times 10^8$ G while the source is in the SP phase (Fig. 3.2a). The observed $\dot{P}_{\rm secular}$ can also be achieved with $B \simeq 1.3 \times 10^8$ G while the source is in the WP phase (Fig. 3.2b). Our results in-

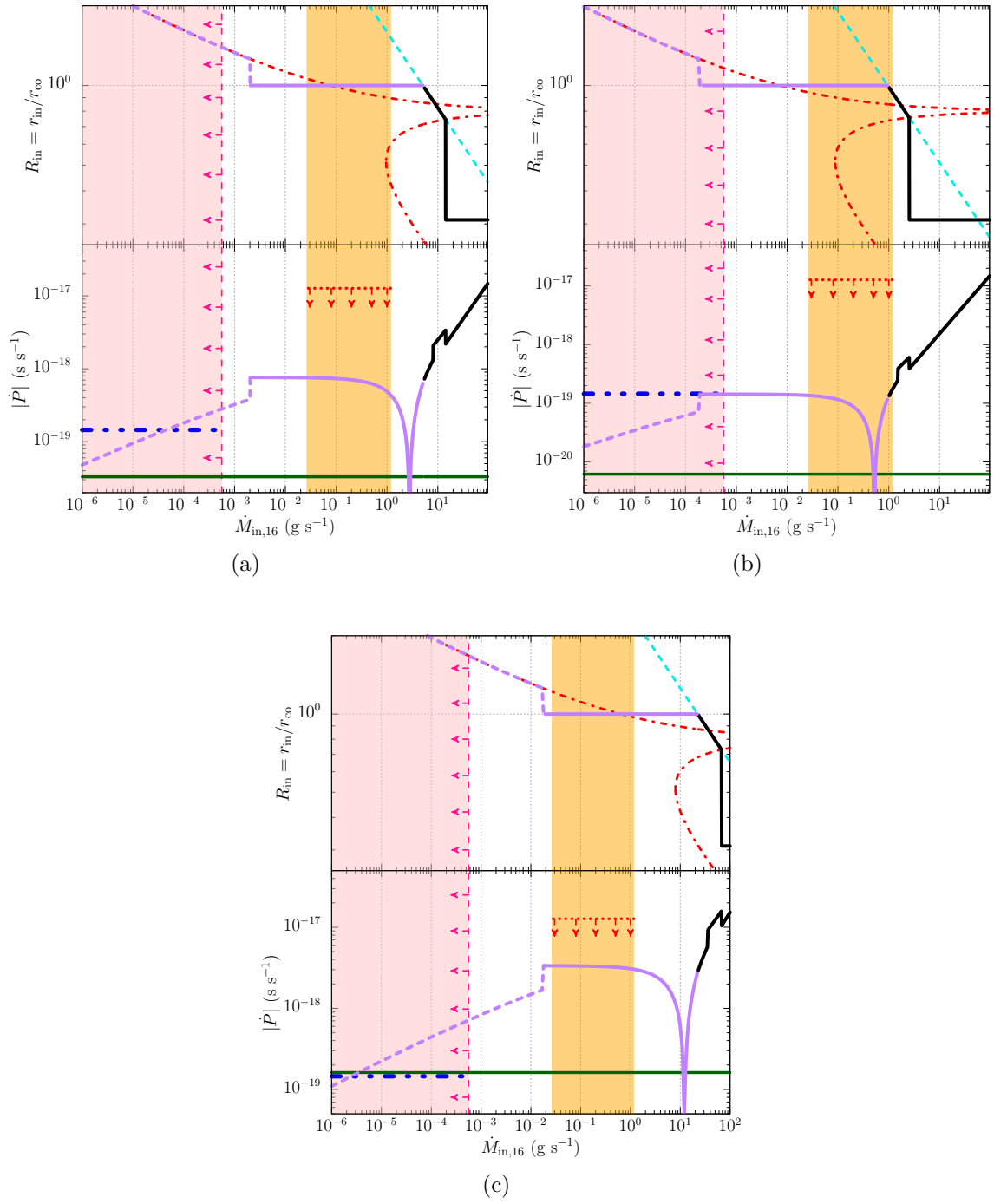

Figure 3.2 The model curves for IGR J17494−3030. (a) The same as Fig. 3.1, but with $P = 2.66$ ms. In the bottom panel, the red arrows represents the upper limit on the $\dot{P}_{\rm outburst}$. These model curves are obtained with $B \simeq 3.0 \times 10^8$ G. (b) The same as (a) except $B \simeq 1.3 \times 10^8$ G. (c) The same as (a) except $B \simeq 6.3 \times 10^8$ G for purely dipole torque (evaporated inner disc) during the quiescent state.

dicate that, the source could be in the WP phase during the outburst state (see Fig. 3.2a), or alternatively, it could be in the SU phase at the beginning of the outburst while 5.2×10^{15} g/s$^{-1} \lesssim \dot{M}_{\rm in} \lesssim 1.2 \times 10^{16}$ g/s^{-1}, and then enters the WP phase as $\dot{M}_{\rm in}$ decreases to $5.2 \times 10^{15} - 2.7 \times 10^{14}$ g/s^{-1} (see Fig. 3.2b).

In the case of evaporated inner disc, the source is estimated to slow down with $B \simeq 6.3 \times 10^8$ G (see Fig. 3.2c). The inner disc forms again with a sharp increase in $\dot{M}_{\rm in}$ taking the source to the WP phase during the outburst.

During the ∼8 years of quiescence, the source spun down by $\Delta P \simeq 3.7 \times 10^{-11}$ s, corresponding to $\dot{P}_{\rm secular} = (1.45 \pm 0.05) \times 10^{-19}$ s s^{-1}. During the ∼8-day outburst, the P changed by $|\Delta P| < 8.8 \times 10^{-12}$ s, corresponding to $|\dot{P}_{\rm outburst}| < 1.27 \times 10^{-17}$ s s^{-1}. This indicates that spin-down during quiescence dominates the rotational evolution of the source.

Our results show that IGR J17494−3030 could be evolving with or without disc during quiescence. Depending on B, the source could enter the SU phase at the beginning of the outburst (see Fig. 3.2b). The $\dot{P}_{\rm outburst}$ measurement could better constrain the models.

3.3 Swift J1756.9–2508

This source was discovered during the 2007 outburst with $P = 5.5$ ms (Krimm et al., 2007; Markwardt et al., 2007). Assuming the source located near the Galactic Centre, its distance is estimated to be 8 kpc (Krimm et al., 2007). The observed properties and the model curves for this source are seen in Fig. 3.3. Similar subsequent outbursts were observed in 2009, 2018, and 2019 (Patruno et al., 2009; Mereminskiy et al., 2018; Sanna et al., 2019). The P value was measured during all the outbursts, and the upper limits on the $\dot{P}_{\rm outburst}$ were obtained for each of them except for the 2019 outburst. In this work, we use the most recent constraint obtained for the 2018 outburst, $|\dot{P}_{\rm outburst}| < 4.22 \times 10^{-17}$ s s^{-1} (Sanna et al., 2018; horizontal dotted line segment with arrows). During this outburst, X-ray pulses were detected in the $L_{\rm X}$ range of $\sim 7.6 \times 10^{35} - 1.53 \times 10^{37}$ erg s^{-1} (Li et al., 2021; orange shaded area in the SU region). $\dot{P}_{\rm secular} = (2.2 \pm 0.78) \times 10^{-20}$ s s^{-1} was estimated from the P measurements during the 2007, 2009, and 2018 outbursts (Bult et al., 2018; horizontal dot-dot-dashed line segment). The upper limit on $L_{\rm X}$ during quiescence was found to be $\sim 1 \times 10^{33}$ erg s^{-1} (Papitto et al., 2007; vertical dashed line with arrows).

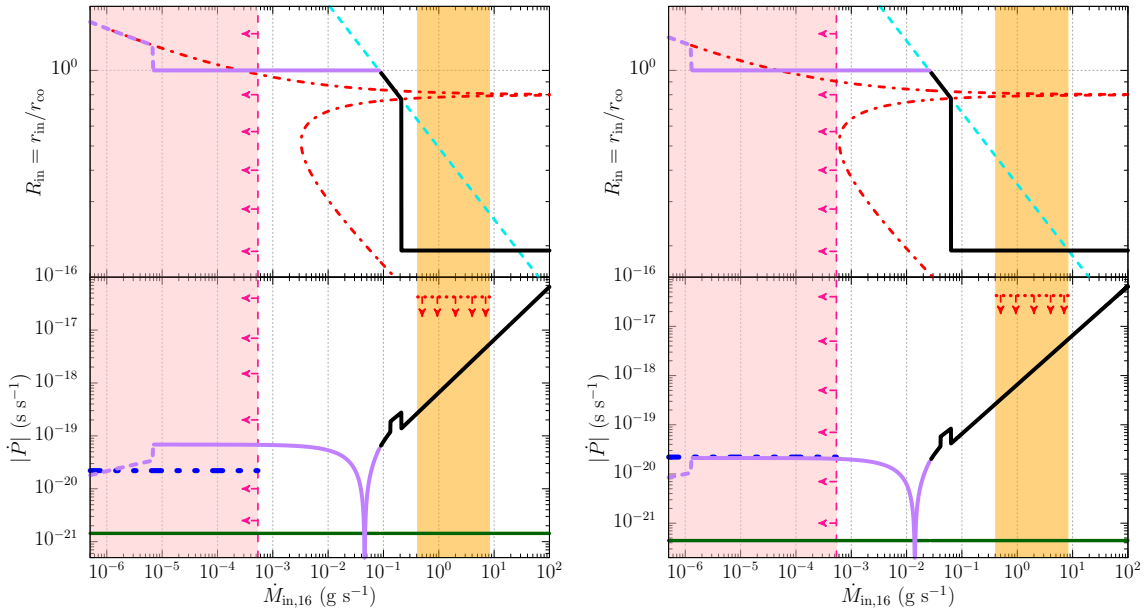

(a) (b)

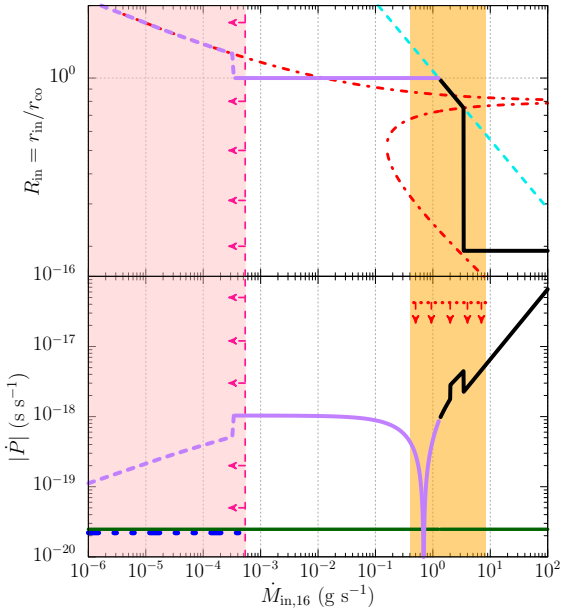

(c)

Figure 3.3 The model curves for Swift J1756.9−2508. (a) The same as Fig. 3.2, but with $P = 5.5$ ms. These model curves are obtained with $B \simeq 9.0 \times 10^7$ G. (b) The same as (a) except $B \simeq 5.0 \times 10^7$ G. (c) The same as (a) except $B \simeq 3.5 \times 10^8$ G and with dipole torque alone in the quiescence.

For the model curves in Fig. 3.3a, the source is in the SP phase during the quiescent state with $B \simeq 9.0 \times 10^7$ G. Fig. 3.3b illustrates the case that the system is in the WP phase with $B \simeq 5.0 \times 10^7$ G during the quiescence. For both cases, we estimate that the source is in the SU phase for the observed range of $L_{\rm X}$ values.

For an evaporated disc during quiescence, reasonable results are obtained with $B \simeq 3.5 \times 10^8$ G (see Fig. 3.3c). With this field strength, the system enters the SU phase during the outburst.

For Swift J1756.9−2508, spin-down during the 11 years between 2007 and 2018 outbursts is approximately $\Delta P \simeq 7.6 \times 10^{-12}$ s, corresponding to $\dot{P}_{\rm secular} = (2.2 \pm 0.78) \times 10^{-20}$ s s^{-1}. For the ∼8 days long 2018 outburst, $|\Delta P| < 2.9 \times 10^{-11}$ s, corresponding to $|\dot{P}_{\rm outburst}| < 4.22 \times 10^{-17}$ s s^{-1}. Considering the actual spin-up values are likely smaller than the upper limits, spin-up and spin-down effects are compatible. As clearly shown in fig. 6 of Sanna et al. (2018), the long-term evolution of the source indicates a net spin-down.

Our results for Swift J1756.9–2508 are reasonable with or without evaporation of the inner disc during the quiescence. Detection of the source in X-rays could better constrain the model. If the quiescent $L_{\rm X}$ level is close to the upper limit ($\sim 10^{33}$ erg s^{-1}), the source is likely to be in the WP phase, where $L_{\rm X} = L_{\rm acc}$. If $L_{\rm X}$ is significantly lower ($\sim 10^{30}$ erg s^{-1}), model curves either indicate the SP phase or the evaporation of the inner disc for the source. However, at such low $\dot{M}_{\rm in}$ levels or beyond, disc evaporation is more likely. For the outburst state, all the estimated B values corresponding to three different cases are in agreement with the $\dot{P}_{\rm outburst}$ upper limit for the observed $L_{\rm X}$ range.

3.4 IGR J17511–3057

This source first detected with $P = 4.1$ ms during the 2009 outburst (Baldovin et al., 2009; Markwardt et al., 2009). Similar subsequent outbursts were observed in 2015 and 2025 (Bozzo et al., 2015; Sguera, 2025). An upper limit of 6.9 kpc on the distance to the source was estimated from the type-I bursts observed during the 2009 outburst (Altamirano et al., 2010). Its observed properties and the model curves are seen in Fig. 3.4. Although X-ray pulses were detected in all three outbursts, $\dot{P}_{\rm outburst}$ was measured only during the 2009 outburst as $-(2.42 \pm 0.3) \times 10^{-18}$ s s^{-1} (horizontal dotted line segment) during which $L_{\rm X}$ decreased from $\sim 1.1 \times 10^{37}$ erg s^{-1} to ∼

3.0×10^{36} erg s^{-1} (Riggio et al., 2011b; orange shaded area in the SU region). In the 2015 outburst, due to the short duration of observation, $\dot{P}$ could not be measured (Papitto et al., 2016). Pulsations were also detected approximately 21 days after the onset of the 2025 outburst, when the source had a low $L_{\rm X} \sim 1.4 \times 10^{34}$ (Illiano et al., 2025; orange vertical line). From the P measurements during the 2009, 2015, and 2025 outbursts without accounting for the transient spin-up episodes during these outbursts, $\dot{P}_{\rm secular} = (3.83 \pm 1.83) \times 10^{-20}$ s s^{-1} (Sanna et al., 2025; horizontal blue line segment). For the quiescent state, $L_{\rm X}$ was found to be $\sim (4.39 \pm 0.85) \times 10^{32}$ erg s^{-1} based on archival Chandra observation from 2009. (Illiano et al., 2025; pink shaded area in the left).

$L_{\rm X}$ of this source has been measured during the quiescence. This $L_{\rm X}$ range provides a better constraint on the current evolutionary phase of the source. For the corresponding $\dot{M}_{\rm in}$ values, the model results indicate that the source cannot be in the SP phase during the quiescent state, a representative illustration with $B \simeq 1.1 \times 10^8$ G can be seen in Fig. 3.4a. The source properties during the quiescence can only be reproduced in the SP phase for η values very close to unity. The source properties can be reproduced in the WP phase with $B \simeq 7.0 \times 10^7$ G (Fig. 3.4b) during the quiescence. For both possibilities, with a sharp increase in the $\dot{M}_{\rm in}$, the source enters the SU phase in the outburst state. Only for this source, X-ray pulsations were detected after the outburst state, at a low $L_{\rm X}$ value corresponding to an $\dot{M}_{\rm in}$ of 7.5×10^{13} g s^{-1}. According to the analytical model, at this $\dot{M}_{\rm in}$ level, the source is in the WP phase, where accretion is possible from the $r_{\rm co}$.

For the case of evaporated disc during the quiescent state, the illustrative model curves seen in Fig. 3.4c are consistent with the measured $\dot{P}_{\rm secular}$ with $B \simeq 4.0 \times 10^8$ G. During the outburst state, the source enters the SU phase with increasing $\dot{M}_{\rm in}$ and subsequently the WP phase as $\dot{M}_{\rm in}$ decreases. For this case also, $\dot{M}_{\rm in}$ value at which pulsations were observed after the outburst corresponds to the WP phase in our model. In this case, the model reproduces the measured average $\dot{P}_{\rm outburst}$ value more accurately.

For about a 10 years of quiescence, this source showed a spun down of $\Delta P \simeq 7.3 \times 10^{-12}$ s, corresponding to $\dot{P}_{\rm secular} = 3.83 \times 10^{-20}$ s s^{-1}. During the $\sim$23 days long outburst, P decreased by $\Delta P \simeq -4.8 \times 10^{-12}$ s, corresponding to $\dot{P}_{\rm outburst} = -(2.42 \pm 0.3) \times 10^{-18}$ s s^{-1}. This indicates that spin-up torque during the outburst was compensated by the spin down in the quiescent state.

For IGR J17511–3057, our results eliminate the SP phase and favour the WP phase or the truncation of the inner disc during quiescence. The model results in the outburst state are compatible with the observations and reproduce the observed

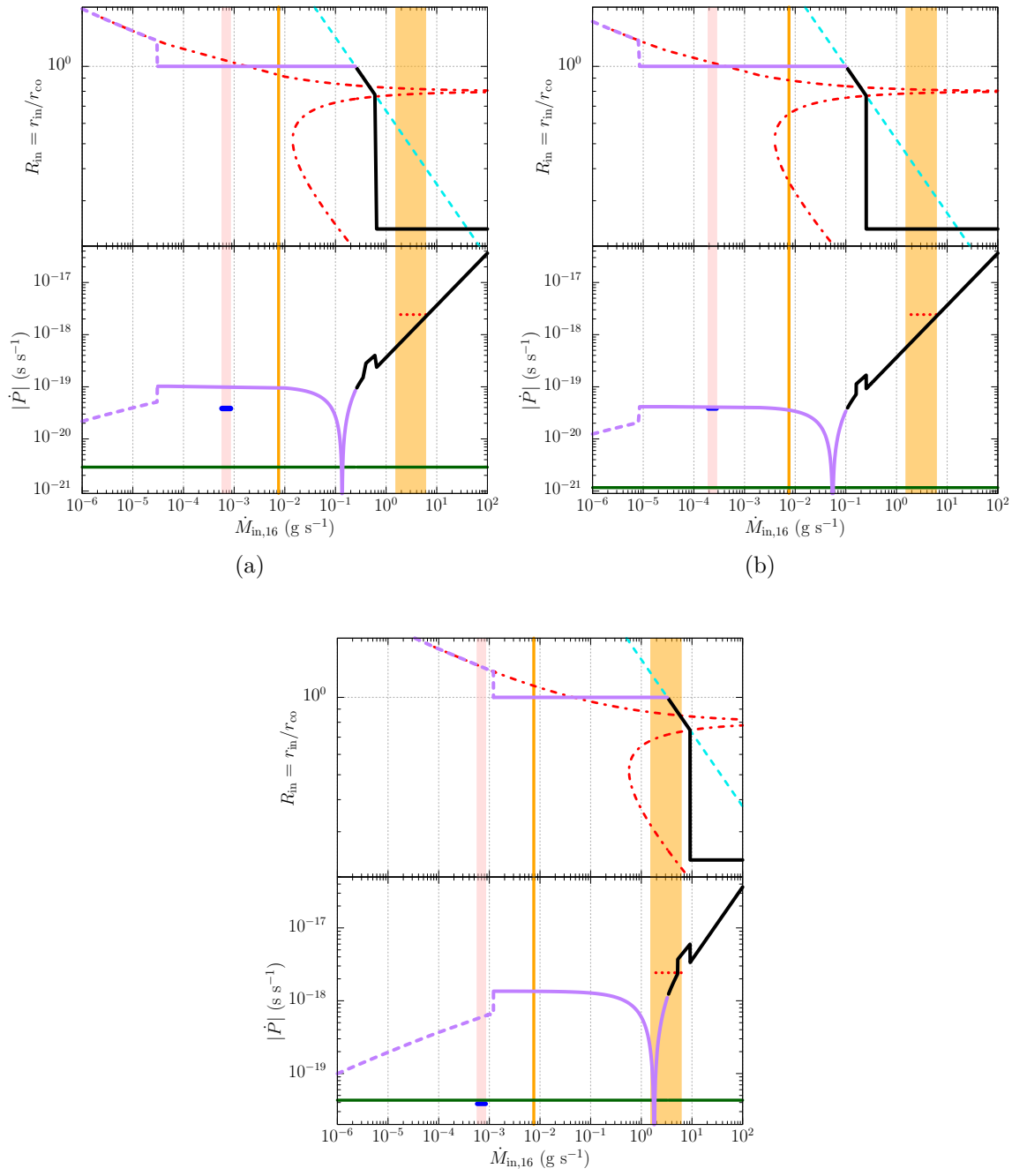

Figure 3.4 The model curves for IGR J17511−3057. (a) The same as Fig. 3.1, but with $P = 4.1$ ms. The orange vertical line represents the $L_{\rm X}$ value at which pulsations were observed. These model curves are obtained with $B \simeq 1.1 \times 10^8$ G. (b) The same as (a) except $B \simeq 7.0 \times 10^7$ G. (c) The same as (a) except $B \simeq 4.0 \times 10^8$ G obtained for dipole torque only in the quiescent state.

$\dot{P}_{\rm outburst}$. The model can reproduce the observed pulsations at low $\dot{M}_{\rm in}$ levels within the considered B range for the source.

3.5 IGR J00291+5934

This source was discovered in 2004 as the fastest known AMXP with $P = 1.7$ ms (Eckert et al., 2004; Markwardt et al., 2004). The source exhibited three more outbursts; two in 2008 separated by ~ 30 days, each reaching roughly half the peak luminosity of the 2004 outburst; ($\sim 3.8 \times 10^{36}$ g s^{-1}) with durations of 9 to 15 days and the third in 2015, which was brightest ($\sim 9.8 \times 10^{36}$ g s^{-1}) with durations of 25 days (Chakrabarty et al., 2008; Patruno, 2010; Sanna et al., 2015; De Falco et al., 2017). The distance to the source was estimated to be 4.2 ± 0.5 kpc from PRE during the type-I burst observed in the 2015 outburst (De Falco et al., 2017). Its observed properties and the model curves are seen in Fig. 3.5. The P and $\dot{P}_{\rm outburst}$ values were measured in all outbursts (Patruno, 2010; Sanna et al., 2017). In this work, we only use the $\dot{P}_{\rm outburst}$ of the 2004 outburst, since the 2008 outbursts were unusual and the timing analysis of the 2015 outburst was not cover the full outburst (Sanna et al., 2017). The X-ray pulsations during 2004 outburst were observed within the $L_{\rm X}$ range of $\sim 3.27 \times 10^{35} - 8.05 \times 10^{36}$ erg s^{-1} (Galloway et al., 2005; orange shaded area in the SU region). For this $L_{\rm X}$ range, $\dot{P}_{\rm outburst} = -(1.42 \pm 0.08) \times 10^{-18}$ s s^{-1} (Patruno, 2010; Papitto et al., 2011; horizontal dotted line segment). During quiescence from the end of the 2004 to the beginning of the first 2008 outburst, $\dot{P}_{\rm secular} = (1.14 \pm 0.33) \times 10^{-20}$ s s^{-1} (Papitto et al., 2011; horizontal dot-dot-dashed line segment). During the quiescence, $L_{\rm X} \approx (2.6 \pm 1.6) \times 10^{32}$ erg s^{-1} (Jonker et al., 2005; pink shaded area in the left).

For IGR J00291+5934, $L_{\rm X}$ have been measured during the quiescent state. For the measured $L_{\rm X}$ range during quiescence, the model results indicate that the source cannot be in the SP phase. An illustration corresponding to this case, with $B \simeq 6.0 \times 10^7$G, can be seen in Fig. 3.5a. The source's properties during quiescence can be explained in the WP phase with $B \simeq 3.7 \times 10^7$G, as illustrated in Fig. 3.5b. In the outburst state, the source enters the SU phase, but the $\dot{P}$ values produced by the model are approximately an order of magnitude lower than the observed $\dot{P}_{\rm outburst}$.

It can be seen in Fig. 3.5c, in the case of the inner disc evaporation during quiescence $\dot{P}_{\rm secular}$ can be reproduced with $B \simeq 1.4 \times 10^8$ G. During the outburst, inner disc

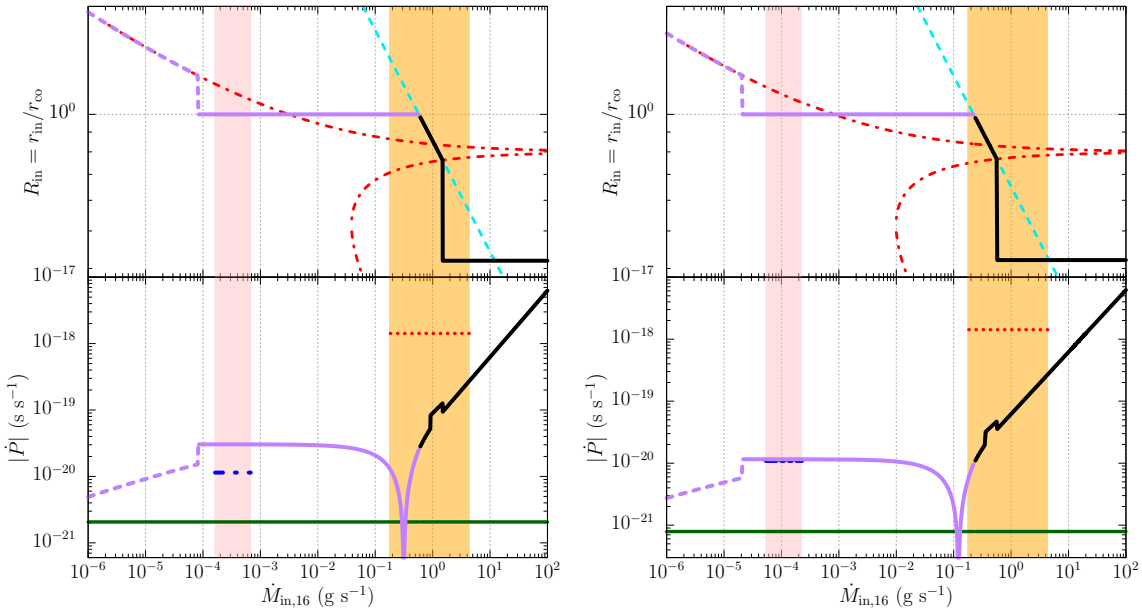

(a) (b)

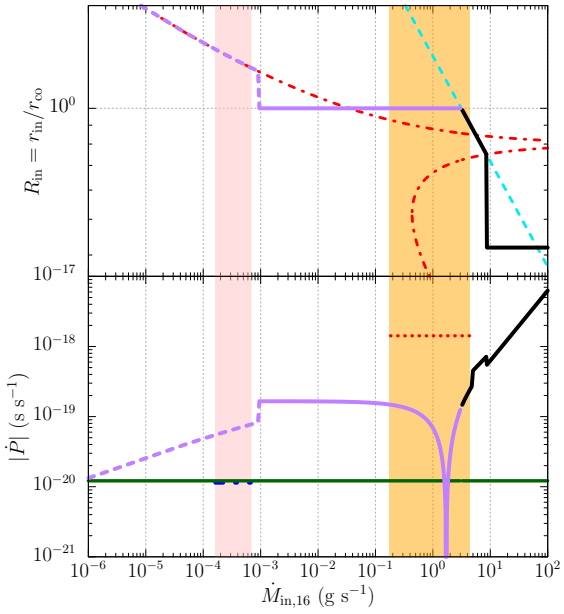

(c)

Figure 3.5 The model curves for IGR J00291+5934. (a) The same as Fig. 3.1, but with $P = 1.7$ ms. These model curves are obtained with $B \simeq 6.0 \times 10^7$ G. (b) The same as (a) except $B \simeq 3.7 \times 10^7$ G. (c) The same as (a) except $B \simeq 1.4 \times 10^8$ G calculated for a purely dipole torque in quiescence.

reforms and the source enters the SU phase for a narrow $\dot{M}_{\rm in}$ range and subsequently the WP phase while $\dot{M}_{\rm in}$ decreases. Also in this case, the model results are not consistent with the observed $\dot{P}_{\rm outburst}$ (see Fig. 3.5c).

During the $\sim$4 years of quiescence, this source showed a spin-down of $\Delta P = 1.4 \times 10^{-12}$ s, corresponding to $\dot{P}_{\rm secular} = (1.14 \pm 0.33) \times 10^{-20}$ s s^{-1}. For about a $\sim$14 days long outburst, P decreased by $\Delta P = -1.7 \times 10^{-12}$ s, corresponding to $\dot{P}_{\rm outburst} = -(1.42 \pm 0.08) \times 10^{-18}$ s s^{-1}. This indicates that the spin down during quiescence compensates for the spin-up torque during the outburst state.

Our results eliminate the SP phase for IGR J00291+5934 and favour the WP phase or the evaporation of the inner disc during the quiescent state. The model curves obtained with different B values, estimated for these separate cases to explain the quiescent-state properties fail to reproduce the observed outburst-state properties. We note that for the 2004 outburst, the measured $\dot{P}_{\rm outburst}$ varied significantly depending on how the data were segmented. Measured $\dot{P}$ increased as $\dot{M}_{\rm in}$ decreases, contradicting the accretion theory (Patruno, 2010). Also, for the 2015 outburst of the source, $\dot{P}_{\rm outburst} = 8.4 \times 10^{-18}$ s s^{-1}, approximately six times greater than the 2004 outburst (Sanna et al., 2017). A more precise measurement is needed to better understand the inconsistency of the model results with the observed values.

4. DISCUSSION

We have investigated the $L_{\rm X}$ and the torque variations of the five AMXPs during their outburst and quiescent states. We have employed the analytical model applied earlier to the torque luminosity relations, torque reversals, and pulsed/non-pulsed X-ray emission properties of LMXBs (Ertan 2021; Gençali et al. 2022; Niang et al. 2024). Our results indicate that the magnetic torques arising from disc-field interaction, magnetic dipole torques, both are spin-down torques, and the spin-up torques associated with the accretion on to the neutron star are sufficient to explain the long-term spin-down behaviour of these systems without requiring any additional torques.

There are other torque models that estimate spin-down torques much weaker than in our model, which necessitate additional spin-down torques to account for the observed long-term net torque acting on AMXPs. In the model used in this work, the magnitude of the spin-down torque in the quiescent state is smaller and comparable to that of spin-up torque in the outburst states. This naturally explains long-term spin-down of these systems, since the quiescent states are much longer than the outburst states. Even if the spin-up torques could be stronger than in our model as proposed by Bhattacharyya & Chakrabarty (2017), this is not sufficient to require additional torques. The most important property of LMXBs to test the models in this concept is their torque reversal behaviour. It is a long-lasting problem to explain the torque reversals of LMXBs with similar torque magnitude on either state of the reversal which occurs with a small variation in $L_{\rm X}$ (Bildsten et al., 1997).

For a given B, illustrative model curves produced with different P values are presented in Fig. 4.1. It is seen that the morphology of the torque reversals are similar for sources with rather different critical $\dot{M}_{\rm in}$ levels corresponding to the torque reversals. Note that the torque reversal occurs with a small change in $\dot{M}_{\rm in}$. This morphology predicted in the model is in good agreement with the torque reversal of 4U 1626-67 (Gençali et al., 2022). For comparison, dashed lines show the $|\dot{P}|$ variation with $\dot{M}_{\rm in}$ estimated in Bhattacharyya & Chakrabarty (2017). It is seen that the torque magnitude estimated in our model is orders of magnitude greater. Several

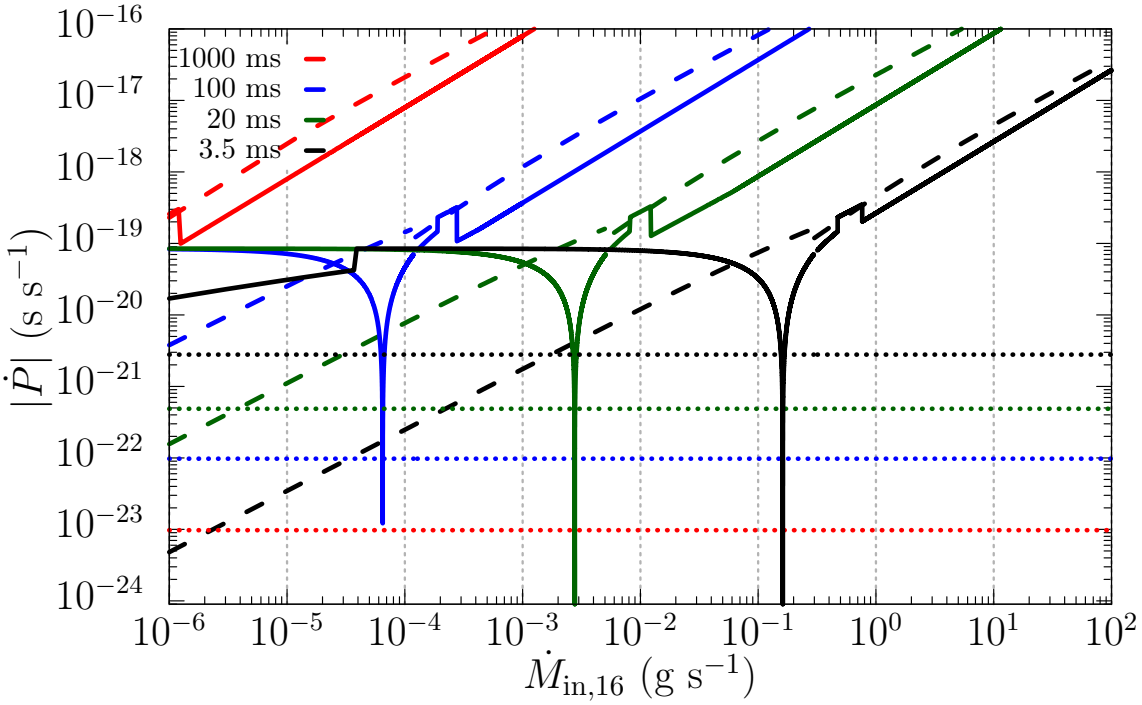

Figure 4.1 The model curves are produced with $B = 1.0 \times 10^8$ G. The solid curves are produced using the analytical model described in Chapter 2. The dotted horizontal lines represent the $\dot{P}$ values when only $\Gamma_{\rm dip}$ is the active torque. The dashed curves are obtained using the torque formulas employed by Bhattacharyya & Chakrabarty (2017).

times stronger average spin-up torque during the outburst leads to a decrease in P which is dominated by the increase during much longer quiescent states, resulting in net long-term spin-down in agreement with the observations. Relatively stronger spin-down torque at a similar level for a large range of $\dot{M}_{\rm in}$ is due to the property of the WP phase with $r_{\rm in} = r_{\rm co}$, for which the magnetic (disc) torque is constant and dominates the accretion torque for that range of $\dot{M}_{\rm in}$ (see Ertan 2021 for details). In this model, the long-term evolution of AMXPs can be explained by the dipole, disc, and accretion torques.

Pulsed radio emission was observed from three tMSPs which show transitions between the X-ray pulsar and the radio pulsar states. The other AMXPs have not been observed to show radio pulses in the quiescent states. In our model, the inner disc radius, and thus the critical accretion rate for the WP/SP transition depends on P, unlike in conventional models, as well as $\dot{M}_{\rm in}$ and B. The critical $\dot{M}_{\rm in}$ for this transition predicted in Ertan (2017, 2018) is in agreement with the transition properties of tMSPs. Estimated critical $\dot{M}_{\rm in}$ levels, which is not achieved in other AMXPs are discussed in Ertan (2018).

Our results imply that sources could be in either the SP (no accretion) or WP (ongoing mass accretion) phase during the quiescent state. The model do not eliminate

the possibility that the inner disc could be evaporated in the quiescence. The lack of radio pulses in the absence of mass accretion might be caused by spherical like geometry of the evaporated disc matter, which could allow some matter to reach to polar caps quenching the radio emission mechanism. In the case of SP phase in the quiescence, the pulsed radio emission is allowed, and there are some ideas to account for the lack of radio pulses for these sources. It was proposed that the radiation pressure from the pulsar may eject most of the matter transferred from the companion, forming a strong wind, which prevents the detection of radio signals through free-free absorption (Burderi et al., 2001). Other possibilities include an unfavourable geometry of the radio beams to the observer or the low radio luminosities below detection limits (Di Salvo & Sanna, 2022).

5. CONCLUSION

In this work, we have investigated the long-term evolution of AMXPs using the comprehensive analytical torque model developed by Ertan (2021). For five AMXPs, measured $\dot{P}_{\rm secular}$ and $\dot{P}_{\rm outburst}$ values show that these sources slow down in the long-term. During the quiescent state, our results indicated that the sources could be in either the SP phase (no accretion), or in the WP phase (accretion with spin-down) depending on the values of B, $\dot{M}_{\rm in}$, and P. In both phases, the disc torque is the dominant torque. We also consider the possibility of the inner disc evaporation due to thermal instabilities at low $\dot{M}_{\rm in}$ levels in the quiescent state. In this case, the source evolves with magnetic dipole torques alone in the quiescent state. For both the outburst and quiescent states, our model results are in agreement with the rotational properties and X-ray luminosities of these AMXPs. This implies that dipole and disc torques are sufficient to account for the observed long-term spin-down of these sources without requiring any additional external spin-down torque mechanism. We have found that the spin-up by accretion torques during the short outburst cannot compensate the spin-down during the much longer quiescent state, resulting in a net spin-down in their long-term evolution. In future works, we aim to develop a time-dependent model to investigate the long-term evolution of the transient sources with different outburst and quiescent state properties.

BIBLIOGRAPHY

Alpar, M. A., Cheng, A. F., Ruderman, M. A., & Shaham, J. (1982). A new class of radio pulsars. *Nature*, *300*, 728–730.

Altamirano, D., Watts, A., Linares, M., Markwardt, C. B., Strohmayer, T., & Patruno, A. (2010). Type I X-ray bursts and burst oscillations in the accreting millisecond X-ray pulsar IGR J17511-3057. *Monthly Notices of the Royal Astronomical Society*, *409*, 1136–1145.

Armas Padilla, M., Wijnands, R., & Degenaar, N. (2013). XMM-Newton and Swift spectroscopy of the newly discovered very faint X-ray transient IGR J17494-3030. *Monthly Notices of the Royal Astronomical Society: Letters*, *436*.

Baade, W. & Zwicky, F. (1934). Remarks on Super-Novae and Cosmic Rays. *Physical Review*, *46*, 76.

Baldovin, C., Kuulkers, E., Ferrigno, C., Bozzo, E., Chenevez, J., Brandt, S., Beckmann, V., Bird, A., Domingo, A., Ebisawa, K., Jonker, P., Kretschmar, P., Markwardt, C., Oosterbroek, T., Paizis, A., Risquez, D., Sanchez-Fernandez, C., Shaw, S., & Wijnands, R. (2009). INTEGRAL discovered a new hard X-ray source: IGRJ17511-3057. *The Astronomer's Telegram, No.2196*, *2196*, 1.

Bhattacharyya, S. & Chakrabarty, D. (2017). The Effect Of Transient Accretion On The Spin-up Of Millisecond Pulsars. *The Astrophysical Journal*, *835*, 4.

Bildsten, L., Chakrabarty, D., Chiu, J., Finger, M. H., Koh, D. T., Nelson, R. W., Prince, T. A., Rubin, B. C., Scott, D. M., Stollberg, M., Vaughan, B. A., Wilson, C. A., & Wilson, R. B. (1997). Observations of Accreting Pulsars. *The Astrophysical Journal Supplement Series*, *113*, 367–408.

Boissay, R., Chenevez, J., Bozzo, E., Ferrigno, C., Grinberg, V., Wilms, J., Caballero, I., Cadolle-Bel, M., Santo, M. D., Fiocchi, M., Kuiper, L., Paizis, A., Sidoli, L., Puehlhofer, G., Sguera, V., Watanabe, K., Enright, J., Graham, E., Jacob, K., & Rusk, D. (2012). A new hard X-ray transient discovered by INTEGRAL: IGR J17494-3030. *The Astronomer's Telegram*, *3984*, 1.

Bozzo, E., Kuulkers, E., Bazzano, A., Beckmann, V., Bird, T., Bodaghee, A., Chenevez, J., Santo, M. D., Domingo, A., Jonker, P., Kretschmar, P., Markwardt, C., Paizis, A., Pottschmidt, K., Sanchez-Fernandez, C., Wijnands, R., Ferrigno, C., & Tuerler, M. (2015). INTEGRAL detects a new outburst from the millisecond X-ray pulsar IGR J17511-3057. *The Astronomer's Telegram, No.7275*, *7275*, 1.

Bult, P., Altamirano, D., Arzoumanian, Z., Chakrabarty, D., Gendreau, K. C., Guillot, S., Ho, W. C. G., Jaisawal, G. K., Lentine, S., Markwardt, C. B., Ngo, S. N., Pope, J. S., Ray, P. S., Saylor, M. R., & Strohmayer, T. E. (2018). On the 2018 Outburst of the Accreting Millisecond X-Ray Pulsar Swift J1756.9–2508 As Seen with NICER. *The Astrophysical Journal*, *864*, 14.

Burderi, L., Possenti, A., Antona, F. D. ., Salvo, T. D., Burgay, M., Stella, L., Menna, M. T., Iaria, R., Campana, S., & D'amico, N. (2001). Where May Ultrafast Rotating Neutron Stars Be Hidden? *The Astrophysical Journal*, *560*, 71–74.

Burderi, L., Salvo, T. D., Menna, M. T., Riggio, A., & Papitto, A. (2006). Order in the Chaos: Spin-up and Spin-down during the 2002 Outburst of SAX J1808.4-3658. *The Astrophysical Journal*, *653*, L133–L136.

Cameron, A. G. W. (1959). Neutron Star Models. *The Astrophysical Journal*, *130*, 884.

Chadwick, J. (1932). Possible existence of a neutron. *Nature*, *129*, 312.

Chakrabarty, D., Jonker, P. G., & Markwardt, C. B. (2013). 2012 Chandra Non-Detection of the Fading X-ray Transient IGR J17494-3030. *The Astronomer's Telegram*, *4886*, 1.

Chakrabarty, D., Swank, J. H., Markwardt, C. B., & Smith, E. (2008). Accreting Millisecond Pulsar IGR J00291-5934 in Outburst Again. *The Astronomer's Telegram, No.1660*, *1660*, 1.

Çoban, O. F. & Ertan, Ü. (2024). Typical X-Ray Outburst Light Curves of Aql X-1. *The Astrophysical Journal*, *961*, 252.

D'Angelo, C. R. (2017). Spin equilibrium in strongly magnetized accreting stars. *Monthly Notices of the Royal Astronomical Society*, *470*, 3316–3331.

Davidson, K. & Ostriker, J. P. (1973). Neutron-Star Accretion in a Stellar Wind: Model for a Pulsed X-Ray Source. *The Astrophysical Journal*, *179*, 585–598.

De Falco, V., Kuiper, L., Bozzo, E., Galloway, D. K., Poutanen, J., Ferrigno, C., Stella, L., & Falanga, M. (2017). The 2015 outburst of the accretion-powered pulsar IGR J00291+5934: INTEGRAL and Swift observations. *Astronomy and Astrophysics*, *599*.

Di Salvo, T. & Sanna, A. (2022). Accretion Powered X-ray Millisecond Pulsars. In S. Bhattacharyya, A. Papitto, & D. Bhattacharya (Eds.), *Millisecond Pulsars* (pp. 87–124). Cham: Springer International Publishing.

Dubus, G., Lasota, J. P., Hameury, J. M., & Charles, P. (1999). X-ray irradiation in low-mass binary systems. *Monthly Notices of the Royal Astronomical Society*, *303*, 139–147.

Eckert, D., Walter, R., Kretschmar, P., Mas-Hesse, M., Palumbo, G. G. C., Roques, J. P., Ubertini, P., & Winkler, C. (2004). IGR J00291+5934, a new X-ray transient discovered with INTEGRAL. *The Astronomer's Telegram, No.352*, *352*, 1.

Ertan, Ü. (2017). The inner disc radius in the propeller phase and accretion-propeller transition of neutron stars. *Monthly Notices of the Royal Astronomical Society*, *466*, 175–180.

Ertan, Ü. (2018). Accretion and propeller torque in the spin-down phase of neutron stars: The case of transitional millisecond pulsar PSR J1023+0038. *Monthly Notices of the Royal Astronomical Society: Letters*, *479*, L12–L16.

Ertan, Ü. (2021). On the torque reversals of accreting neutron stars. *Monthly Notices of the Royal Astronomical Society*, *500*, 2928–2936.

Frank, J., King, A., & Raine, D. J. (2002). Accretion Power in Astrophysics: Third Edition. *Cambridge University Press*, *39*, 398.

Galloway, D. K., Markwardt, C. B., Morgan, E. H., Chakrabarty, D., & Strohmayer, T. E. (2005). Discovery of the Accretion-powered Millisecond X-Ray Pulsar IGR J00291+5934. *The Astrophysical Journal*, *622*, L45–L48.

Gamow, G. & Teller, E. (1936). Selection Rules for the β Disintegration. *Physical Review*, *49*, 895.

Gençali, A. A., Niang, N., Toyran, O., Ertan, Ü., Ulubay, A., Şaşmaz, S., Devlen, E., Vahdat, A., Özcan, & Alpar, M. A. (2022). The torque reversals of 4U 1626–67. *Astronomy and Astrophysics*, *658*, A13.

Ghosh, P. & Lamb, F. K. (1979). Accretion by rotating magnetic neutron stars. III. Accretion torques and period changes in pulsating X-ray sources. *The Astrophysical Journal*, *234*, 296–316.

Giacconi, R., Gursky, H., Kellogg, E., Schreier, E., & Tananbaum, H. (1971). Discovery of Periodic X-Ray Pulsations in Centaurus X-3 from UHURU. *The Astrophysical Journal*, *167*, L67.

Giacconi, R., Gursky, H., Paolini, F. R., & Rossi, B. B. (1962). Evidence for X Rays From Sources Outside the Solar System. *Physical Review Letters*, *9*, 439–443.

Gierliński, M. & Poutanen, J. (2005). Physics of accretion in the millisecond pulsar XTE J1751-305. *Monthly Notices of the Royal Astronomical Society*, *359*, 1261–1276.

Haskell, B., Degenaar, N., & Ho, W. C. (2012). Constraining the physics of the r-mode instability in neutron stars with X-ray and ultraviolet observations. *Monthly Notices of the Royal Astronomical Society*, *424*, 93–103.

Hewish, A., Bell, S. J., Pilkington, J. D., Scott, P. F., & Collins, R. A. (1968). Observation of a Rapidly Pulsating Radio Source. *Nature*, *217*, 709–713.

Illiano, G., Papitto, A., Campana, S., Marino, A., Zanon, A. M., Carotenuto, F., Zelati, F. C., Baglio, M. C., Ambrosino, F., Malacaria, C., Ballocco, C., Jaisawal, G. K., Messa, M. M., Parent, E., Russell, T. D., Sanna, A., & Tzioumis, A. (2025). Detection of low-luminosity X-ray pulsations from the accreting millisecond pulsar IGR J17511-3057: an ever-thinning thread between bright accretion and sub-luminous states. *Astronomy and Astrophysics*, arXiv:2507.13248.

Jonker, P. G., Campana, S., Steeghs, D., Torres, M. A., Galloway, D. K., Markwardt, C. B., Chakrabarty, D., & Swank, J. (2005). Chandra observations of the millisecond X-ray pulsar IGR J00291+5934 in quiescence. *Monthly Notices of the Royal Astronomical Society*, *361*, 511–516.

Krimm, H. A., Markwardt, C. B., Deloye, C. J., Romano, P., Chakrabarty, D., Campana, S., Cummings, J. R., Galloway, D. K., Gehrels, N., Hartman, J. M., Kaaret, P., Morgan, E. H., & Tueller, J. (2007). Discovery of the Accretion-powered Millisecond Pulsar SWIFT J1756.9-2508 with a Low-Mass Companion. *The Astrophysical Journal*, *668*, L147–L150.

Lasota, J. P. (2001). The disc instability model of dwarf novae and low-mass X-ray binary transients. *New Astronomy Reviews*, *45*, 449–508.

Li, Z. S., Kuiper, L., Falanga, M., Poutanen, J., Tsygankov, S. S., Galloway, D. K., Bozzo, E., Pan, Y. Y., Huang, Y., Zhang, S. N., & Zhang, S. (2021). Broadband X-ray spectra and timing of the accreting millisecond pulsar Swift J1756.9-2508 during its 2018 and 2019 outbursts. *Astronomy and Astrophysics*, *649*.

Manchester, R. N., Hobbs, G. B., Teoh, A., & Hobbs, M. (2005). The Australia Telescope National Facility Pulsar Catalogue. *The Astronomical Journal*, *129*, 1993–2006.

Markwardt, C. B., Altamirano, D., Strohmayer, T. E., & Swank, J. H. (2009). RXTE and Swift: IGR J17511-3057 fading, XTE J1751-305 detected. *The Astronomer's Telegram, No.2237*, *2237*, 1.

Markwardt, C. B., Krimm, H. A., & Swank, J. H. (2007). SWIFT J1756.9-2508 is a 182 Hz Millisecond X-ray Pulsar. *The Astronomer's Telegram, No.1108*, *1108*, 1.

Markwardt, C. B., Swank, J. H., & Strohmayer, T. E. (2004). IGR J00291+5934 is a 598 Hz X-ray Pulsar. *The Astronomer's Telegram*, *353*, 1.

Markwardt, C. B., Swank, J. H., Strohmayer, T. E., 't Zand, J. J. M. I., & Marshall, F. E. (2002). DISCOVERY OF A SECOND MILLISECOND ACCRETING PULSAR: XTE J1751-305. *The Astrophysical Journal*, *575*, 21–24.

Mereminskiy, I. A., Grebenev, S. A., Krivonos, R. A., & Sunyaev, R. A. (2018). New X-ray outburst of accreting millisecond pulsar SWIFT J1756.9-2508 detected by INTEGRAL. *The Astronomer's Telegram, No. 11497*, *11497*, 1.

Ng, M., Ray, P. S., Bult, P., Chakrabarty, D., Jaisawal, G. K., Malacaria, C., Altamirano, D., Arzoumanian, Z., Gendreau, K. C., Güver, T., Kerr, M., Strohmayer, T. E., Wadiasingh, Z., & Wolff, M. T. (2021). NICER Discovery of Millisecond X-Ray Pulsations and an Ultracompact Orbit in IGR J17494-3030. *The Astrophysical Journal Letters*, *908*, L15.

Ng, M., Ray, P. S., Strohmayer, T. E., Bult, P. M., Chakrabarty, D., Altamirano, D., Jaisawal, G. K., Malacaria, C., Bogdanov, S., Gendreau, K. C., & Arzoumanian, Z. (2020). NICER detection of 376 Hz X-ray pulsations from IGR J17494-3030. *The Astronomer's Telegram*, *14124*, 1.

Niang, N., Ertan, Ü., Gençali, A. A., Toyran, O., Ulubay, A., Devlen, E., Alpar, M. A., & Gügercinoğlu, E. (2024). On the lack of X-ray pulsation in most neutron star low-mass X-ray binaries. *Monthly Notices of the Royal Astronomical Society*, *532*, 2133–2142.

Oppenheimer, J. R. & Volkoff, G. M. (1939). On Massive Neutron Cores. *Physical Review*, *55*, 374.

Papitto, A., Bozzo, E., Sanchez-Fernandez, C., Romano, P., Torres, D. F., Ferrigno, C., Kajava, J. J., & Kuulkers, E. (2016). The 2015 outburst of the accreting millisecond pulsar IGR J17511-3057 as seen by INTEGRAL, Swift, and XMM-Newton. *Astronomy and Astrophysics*, *596*.

Papitto, A., di Salvo, T., Burderi, L., Gallo, E., Menna, M. T., Riggio, A., Krauss, M. I., Chakrabarty, D., Antonelli, A., Bozzo, E., Burgay, M., D'Amico, N., Israel, R. I. G. L., Possenti, A., & Testa, V. (2007). Chandra non-detection of the newly discovered Millisecond X-ray Pulsar SWIFT J1756.9-2508. *The Astronomer's Telegram, No.1133*, *1133*, 1.

Papitto, A. & Martino, D. d. (2022). Transitional Millisecond Pulsars. In S. Bhattacharyya, A. Papitto, & D. Bhattacharya (Eds.), *Millisecond Pulsars* (pp. 157–200). Cham: Springer International Publishing.

Papitto, A., Menna, M. T., Burderi, L., Salvo, T. D., & Riggio, A. (2008). Measuring the spin up of the accreting millisecond pulsar XTE J1751-305. *Monthly Notices of the Royal Astronomical Society*, *383*, 411–416.

Papitto, A., Riggio, A., Burderi, L., Salvo, T. D., D'Aí, A., & Iaria, R. (2011). Spin down during quiescence of the fastest known accretion-powered pulsar. *Astronomy and Astrophysics*, *528*.

Patruno, A. (2010). The accreting millisecond X-ray pulsar IGR J00291+5934: Evidence for a long timescale spin evolution. *The Astrophysical Journal*, *722*, 909–918.

Patruno, A., Markwardt, C. B., Strohmayer, T. E., Swank, J. H., Smith, S. E., & Pereira, D. (2009). RXTE PCA and Swift BAT detects the Millisecond Pulsar Swift J1756.9-2508 in Outburst. *The Astronomer's Telegram, No.2130*, *2130*, 1.

Patruno, A. & Watts, A. L. (2021). Accreting Millisecond X-ray Pulsars. In T. M. Belloni, M. Méndez, & C. Zhang (Eds.), *Timing Neutron Stars: Pulsations, Oscillations and Explosions* (pp. 143–208). Berlin, Heidelberg: Springer Berlin Heidelberg.

Radhakrishnan, V. & Srinivasan, G. (1982). On the origin of the recently discovered ultra-rapid pulsar. *Curr.Sci.*, *51*, 1096–1099.

Riggio, A., Burderi, L., Salvo, T. D., Papitto, A., D'Aì, A., Iaria, R., & Menna, M. T. (2011a). Secular spin-down of the AMP XTE J1751-305. *Astronomy and Astrophysics*, *531*.

Riggio, A., Papitto, A., Burderi, L., Salvo, T. D., Bachetti, M., Iaria, R., D'Aì, A., & Menna, M. T. (2011b). Timing of the accreting millisecond pulsar IGR J17511-3057. *Astronomy and Astrophysics*, *526*.

Sanna, A., Jaisawal, G. K., Strohmayer, T. E., Illiano, G., Riggio, A., Papitto, A., Salvo, T. D., Burderi, L., Coley, J. B., Altamirano, D., Malacaria, C., Anitra,

A., Ng, M., Chakrabarty, D., Boztepe, T., & Albayati, A. C. (2025). The 2025 outburst of IGR J17511-3057: timing and spectral insights from NICER and NuSTAR. *Astronomy and Astrophysics*.

Sanna, A., Pintore, F., Bozzo, E., Ferrigno, C., Papitto, A., Riggio, A., Salvo, T. D., Iaria, R., D'Aì, A., Egron, E., & Burderi, L. (2017). Spectral and timing properties of IGR J00291+5934 during its 2015 outburst. *Monthly Notices of the Royal Astronomical Society*, *466*, 2910–2917.

Sanna, A., Pintore, F., Riggio, A., Burderi, L., Gambino, A. F., Gendreau, K. C., Arzoumanian, Z., Bult, P. M., di Salvo, T., Iaria, R., Ferrigno, C., Bozzo, E., & Papitto, A. (2019). NICER and SWIFT/XRT detect a new outburst of the accreting millisecond X-ray pulsar SWIFT J1756.9-2508. *The Astronomer's Telegram*, *12882*, 1.

Sanna, A., Pintore, F., Riggio, A., Burderi, L., Salvo, T. D., Iaria, R., Scarano, F., Papitto, A., & Bozzo, E. (2015). Swift detected a renewed X-ray activity in IGR J00291+5934. *The Astronomer's Telegram, No.7836*, *7836*, 1.

Sanna, A., Pintore, F., Riggio, A., Mazzola, S. M., Bozzo, E., Salvo, T. D., Ferrigno, C., Gambino, A. F., Papitto, A., Iaria, R., & Burderi, L. (2018). SWIFT J1756.9-2508: Spectral and timing properties of its 2018 outburst. *Monthly Notices of the Royal Astronomical Society*, *481*, 1658–1666.

Sguera, V. (2025). The onset of a new outburst from the millisecond X-ray pulsar IGR J17511-3057 as detected by INTEGRAL. *The Astronomer's Telegram, No. 17029*, *17029*, 1.

Sterne, T. E. (1933). A note on the liberation of energy by transmutations of nuclei in the stars. *Monthly Notices of the Royal Astronomical Society*, *93*, 767.

Tananbaum, H., Gursky, H., Kellogg, E. M., Levinson, R., Schreier, E., & Giacconi, R. (1972). Discovery of a Periodic Pulsating Binary X-Ray Source in Hercules from UHURU. *The Astrophysical Journal*, *174*, L143.

Wijnands, R., Homan, J., Heinke, C. O., Miller, J. M., & Lewin, W. H. G. (2005). Chandra Observations of the Accretion-driven Millisecond X-Ray Pulsars XTE J0929−314 and XTE J1751−305 in Quiescence . *The Astrophysical Journal*, *619*, 492–502.

Wijnands, R. & van der Klis, M. (1998). A millisecond pulsar in an X-ray binary system. *Nature*, *394*, 344–346.

Woosley, S. E. & Weaver, T. A. (1986). The Physics of Supernova Explosions. *Annual Review of Astronomy and Astrophysics*, *24*, 205–253.

Zel'dovich, Y. B. & Novikov, I. D. (1965). Relativistic Astrophysics I. *Soviet Physics Uspekhi*, *7*, 763.